LUND UNIVERSITY

Optimal Temperature and Pressure Control of the Acid Sulfite Cooking Process

Mårtensson, Krister; Ljung, Lennart; Nilsson, Lars-Olof

1973

Document Version:
Publisher's PDF, also known as Version of record

Link to publication

Citation for published version (APA):
Mårtensson, K., Ljung, L., & Nilsson, L.-O. (1973). *Optimal Temperature and Pressure Control of the Acid Sulfite Cooking Process*. (Technical Reports TFRT-7033). Department of Automatic Control, Lund Institute of Technology (LTH).

Total number of authors:
3

General rights
Unless other specific re-use rights are stated the following general rights apply:
Copyright and moral rights for the publications made accessible in the public portal are retained by the authors and/or other copyright owners and it is a condition of accessing publications that users recognise and abide by the legal requirements associated with these rights.
• Users may download and print one copy of any publication from the public portal for the purpose of private study or research.
• You may not further distribute the material or use it for any profit-making activity or commercial gain
• You may freely distribute the URL identifying the publication in the public portal

Read more about Creative commons licenses: https://creativecommons.org/licenses/

Take down policy
If you believe that this document breaches copyright please contact us providing details, and we will remove access to the work immediately and investigate your claim.

LUND UNIVERSITY

PO Box 117
221 00 Lund
+46 46-222 00 00

Download date: 17. Dec. 2025

TFRT-7033

OPTIMAL TEMPERATURE AND PRESSURE CONTROL OF THE ACID SULFITE COOKING PROCESS

Krister Mårtensson
Lennart Ljung
Lars-Olof Nilsson

Report 7320 Juni 1973
Lund Institute of Technology
Division of Automatic Control

TILLHÖR REFERENSBIBLIOTEKET
UTLÅNAS EJ

REGLERINGSTEKNIK
LTH

OPTIMAL TEMPERATURE AND PRESSURE CONTROL OF THE ACID SULFITE COOKING PROCESS

Krister Mårtensson Lennart Ljung Lars-Olof Nilsson

ABSTRACT.

The determination of efficient temperature and pressure control strategies for a sulfite cooking process is formulated as an optimal control problem. Different cost functionals and constraints are considered, and it is shown that a realistic formulation of the problem results in a singular problem with both control and state variable constraints. Numerical solutions are presented and the computational aspects are thoroughly discussed.

TABLE OF CONTENTS

Table of Contents (Contd.)

1. INTRODUCTION.

Optimal control of dynamic systems has become a well established field in control theory, and theoretical results are available for a large class of problems. However, very few applications to complex industrial or other real-life processes are reported. One contributing factor to this is the difficulties that generally are associated with the numerical solution. Although various algorithms have been suggested, e.g. [1], [3], [4], there is no universally efficient method, and in general each problem has its own inherent difficulties.

The optimal control problem considered here is based on a mathematical model developed by N.-H. Schöön and B. Hagberg for the acid sulfite cooking process [7]. The model is based on known chemical properties as well as on experimental data, and very good agreement has been reported for a laboratory pilot process.

The optimization problems that we formulate and solve for this process turn out to be very complex when all the different technological constraints for the process are considered. Thus, the cooking process is described by five state variables and two control variables (change rates of temperature and partial pressure of sulphur dioxide), and there are constraints on the control as well as on the state variables. Besides, the problem is singular and the differential equations $\dot{x} = f(x,u)$ describing the process have discontinuous right-hand sides.

The numerical algorithm that we use is based on the differential dynamic programming technique [3]. The state variable constraints are handled with the constraining hyperplane technique [4], and the singularity is removed with a modified form of the so called "ε-$\alpha(\cdot)$ algorithm". With

these tools it proves possible to compute the optimal control strategies.

The report is organized as follows. In Section 2 a brief description of the acid sulfite cooking process is given, and a mathematical model is presented. In Section 3 the optimal control problem is formulated. Section 4 deals with the optimization of a simplified problem, where the constraints on control change rates are neglected. In Section 5 the complete set of constraints is considered, and finally in Section 6 the same problem is formulated and solved for a modified model of the process.

2. THE ACID SULFITE COOKING PROCESS.

The different cellulose cooking processes constitute a class of very complex chemical processes. The complete mechanisms of these processes are rather poorly understood, and thus mathematical models based on pure chemical reaction laws have not yet been possible to develop. An alternative approach to the modelling problem is described by N.-H. Schöön and B. Hagberg in [7] where they combine measurements from an acid sulfite cooking process with known chemical properties to describe the quantitative behaviour of the most important reactants. These results have served as a basis for the mathematical model used in this study, and we thus refer to [7] for a comprehensive account for different problems connected to the modelling. In this section we will just summarize the necessary fundamental relations, and give a very brief account of the acid sulfite cooking process.

Roughly, the outcome of the process depends on a few components, namely the cellulose, the lignin and the hemicellulose concentration. The cellulose is obtained through dissolution of the lignin which acts like some kind of glue in the wood-chips, and the dissolution of the lignin can be obtained by chemicals that do not react with the cellulose. Thus the problem to get a certain amount of free cellulose fibres is equivalent to reduction of the lignin content below a certain level. Since the cellulose does not take part in any chemical reaction, the cellulose concentration can then be excluded from the mathematical model. However, the wood-chips also contain different kinds of celluloses that do react with the chemicals. These are lumped together in what is called the hemicellulose content of the chips. The hemicellulose content decreases as the lignin dissolution proceeds, and this is highly unsatisfactory since the hemicellulose as well

as the cellulose may be utilized in the paper production. A desirable quality of the control strategies for the process is thus to reduce the lignin content below a predetermined level in such a way that the hemicellulose reduction is minimized. However, as will be shown below, the lignin and the hemicellulose reduction depend approximately in the same way on the control variables (temperature and pressure). The problem could thus be expected to be well suited for a refined mathematical technique like optimal control theory.

As a first attempt to describe the lignin dissolution, the following structure of the delignification rate equation was assigned.

$$\frac{d}{dt}([L]_o - [L]) = r_L = k_L(T)[L]^m[HSO_3^-]^\alpha[H^+]^\beta \qquad (2.1)$$

$k_L(T)$ is a temperature dependent parameter which is assumed to be of the form $k_L(T) = k_L^o \exp(-E_L/T)$. $[L]$ is the lignin concentration in the wood-chips calculated with respect to the uncooked wood. $[L]_o$ is the initial value. $[HSO_3^-]$ and $[H^+]$ are the concentrations of hydrogen sulfite ions and hydrogen ions at the cooking temperature. m, α and β are exponents (the orders of the reaction) which are assumed to be constant.

The best fit of equation (2.1) to the experiments was found if (2.1) was replaced by two similar equations, one valid above the lignin content 12.42% and the other one valid below 12.42%. The following rate equations were then found.

[L] $\geq$ 12.42%:

$$\begin{cases} r_L = k_L(T)[L]^{0.6463}[HSO_3^-]^{0.8186}[H^+]^{0.7053} \\ k_L(T) = 0.4845 \cdot 10^{16} \cdot \exp(-12495/T) \end{cases} \tag{2.2}$$

[L] $<$ 12.42%:

$$\begin{cases} r_L = k_L(T)[L]^{1.6212}[HSO_3^-]^{0.7647}[H^+]^{0.7794} \\ k_L(T) = 0.1464 \cdot 10^{16} \cdot \exp(-12506/T) \end{cases}$$

The temperature T is in degrees Kelvin and time t is in hours. It can be seen from (2.2) that the reaction order with respect to the lignin content as well as the parameter k_L^o change considerably. The chemical aspects on this phenomenon are discussed in [7], and an explanation based on topochemistry is given. However, from the optimization point of view the split of the rate equation is rather unsatisfactory since it will imply discontinuities in the adjoint variables. Different ways to approximate (2.2) with one smooth equation will thus be discussed in Section 4. Also notice that the rate equations depend on the concentration of hydrogen sulfite ions, $[HSO_3^-]$, as well as the concentration of hydrogen ions, $[H^+]$. These quantities are related to the formation of different acids, and the necessary equations are given below.

The hemicellulose content is in practice a composite of many hemicelluloses with very different properties. When modelling the process, these were lumped together into one quantity [C]. The best fit to the measured reduction of the hemicellulose content was then obtained with the rate equation

$$-\frac{d}{dt}[C] = r_C = k_C(T)[C]^{2.5420}[H^+]^{0.7069} \tag{2.3a}$$

where

$$k_c(T) = 0.4541 \cdot 10^{15} \exp(-14031/T) \qquad (2.3b)$$

The unit of [C] is gram hemicellulose per 100 g uncooked wood.

The paper pulp yield and the lignin content of the pulp are not possible to calculate from eqs. (2.2) and (2.3), since these depend on the hydrogen ion concentration and the hydrogen sulfite ion concentration of the digesting liquor. These concentrations depend in its own turn on the formation of several different acids during the cook [7], and it is very difficult to mathematically describe these different formations. It was thus proposed in [7] and [8] that the concentration of the different strong acids should be lumped together into the quantity $[SA^-]$, and as a first attempt the following relation (Model I) between $[SA^-]$ and the lignin dissolution was considered, [8].

$$[SA^-]v/([L]_o-[L]) = g + h([L]_o-[L]) + \int_0^t k_{SA}([L]_o-[L])^S [HSO_3^-]^\delta [H^+]^\varepsilon d\tau \qquad (2.4a)$$

The parameter k_{SA} is given by

$$k_{SA} = k_{SA}^o \exp(-E_{SA}/T) \qquad (2.4b)$$

and is thus a function of time when the temperature T varies during the cook. The left-hand side of (2.4a) gives the concentration of strong acids per amount of lignin dissolved, and a correction v is introduced for the liquor to wood ratio. The first two terms on the right-hand side give the degree of sulfonation of the dissolved lignin, and the third term gives the formation of sulfonic acids

due to further sulfonation in the digesting liquor. The parameters g, h, k^o_{SA}, E_{SA}, s, δ and ε were determined by fitting (2.4a) to the measurements, and the following numerical values were obtained:

$$\begin{aligned} g &= 0.09703 \\ h &= -0.002584 \\ k^o_{SA} &= 0.2824 \cdot 10^{16} \\ E_{SA} &= 15715 \\ s &= 1.3991 \\ \delta &= 1.5287 \\ \varepsilon &= 0.6903 \\ v &= 4.5 \end{aligned} \qquad (2.5)$$

Notice that these numerical values are of very little interest from a wood chemist's point of view, since many different phenomena are lumped together in (2.4).

To get a differential equation for the formation of strong acids, (2.4) is rewritten as

$$[SA^-] = \frac{g}{v}([L]_o-[L]) + \frac{h}{v}([L]_o-[L])^2 +$$

$$+ \frac{1}{v}([L]_o-[L]) \int_0^t k_{SA}([L]_o-[L])^s[HSO_3^-]^\delta[H^+]^\varepsilon d\tau$$

Then

$$\frac{d}{dt}[SA^-] = \frac{g}{v} r_L + \frac{2h}{v}([L]_o - [L])r_L +$$

$$+ \frac{1}{v} r_L \int_0^t k_{SA}([L]_o - [L])^s [HSO_3^-]^\delta [H^+]^\varepsilon d\tau +$$

$$+ \frac{1}{v}([L]_o - [L])^{s+1} k_{SA} [HSO_3^-]^\delta [H^+]^\varepsilon$$

and thus the rate equation for the formation of strong acids (model I) may be written as

$[L] = [L]_o$:

$$r_{SA} = (g/v) r_L \qquad (2.6)$$

$[L] < [L]_o$:

$$r_{SA} = \left\{[SA^-]/([L]_o - [L]) + (h/v)([L]_o - [L])\right\} r_L +$$

$$+ (k_{SA}/v)([L]_o - [L])^{s+1} [HSO_3^-]^\delta [H^+]^\varepsilon$$

Alternatively, we may consider the quantity $[SA^-]/([L]_o - [L])$. A straightforward differentiation of (2.4a) then yields

$$\frac{d}{dt}\left\{[SA^-]/([L]_o - [L])\right\} = \frac{h}{v} r_L + \frac{k_{SA}}{v}([L]_o - [L])^s [HSO_3^-]^\delta [H^+]^\varepsilon \qquad (2.7a)$$

and the boundary condition is

$$\left\{[SA^-]/([L]_o - [L])\right\}_{t=t_0} = \frac{h}{v}\{r_L\}_{t=t_0} \qquad (2.7b)$$

This reformulation of the problem will later prove to be necessary to do to get a well conditioned optimization problem.

An alternative model (model II) of the formation of strong acids is presented in [6] and [7] . The rate equation

$$r_{SA} = \left\{k_{SA}(T)/v\right\}[SA^-]^a[HSO_3^-]^b[H^+]^c \qquad (2.8a)$$

with

$$k_{SA}(T) = k_{SA}^o \exp(-E_{SA}^s/T) \qquad (2.8b)$$

was fitted to the measurements, and it proved to be slightly more accurate than the relation (2.4). The best fit was obtained with the following values of the parameters.

$$\begin{aligned} k_{SA}^o &= 0.9882 \cdot 10^{12} \\ E_{SA} &= 10484 \\ a &= -0.4296 \\ b &= 0.6248 \\ c &= 0.5537 \end{aligned} \qquad (2.9)$$

Both models are investigated in the optimization study presented below. The main effort was concentrated to the relation (2.4) (model I) since (2.8) (model II) was not available when the study was initiated. However, the model (2.8) is investigated in Section 6, and it is shown that the change of the model has very little influence on the optimal control strategies. Besides, (2.4) results in a somewhat more difficult optimization problem, and (2.4) will thus better illustrate the possibilities of optimal control theory.

Since the rate equations (2.2), (2.3), (2.6), (2.7) and (2.8) depend on the concentration of hydrogen sulfite ions, $[H^+]$, it remains to determine these in terms of the known quantities. According to [7], these concentrations are related to

the formation of strong acids through the electroneutrality condition

$$[Na^+] + [H^+] = [HSO_3^-] + [SA^-] \qquad (2.10)$$

where $[Na^+]$ (=0.375) is the concentration of sodium ions from the ionic medium (sodium chloride). This quantity is measurable, and is kept constant during the cooking through a continuous provision of ionic medium. Finally, the partition of the sulphur dioxide between the liquor and the gas phase is governed by the relation

$$[H^+][HSO_3^-]/p_{SO_2} = K_{p_{SO_2}}(T) \qquad (2.11)$$

where p_{SO_2} is the partial pressure of the sulphur dioxide in the steam and $K_{p_{SO_2}}(T)$ is an equilibrium constant given by

$$^{10}\log K_{p_{SO_2}}(T) = 2665/T - 10.208 \qquad (2.12)$$

If the control variables are chosen as the partial pressure p_{SO_2} and the temperature T, it is clear from (2.10) and (2.11) that $[H^+]$ and $[HSO_3^-]$ may be expressed in terms of the control variables and the strong acid concentration $[SA^-]$. Alternatively, we may consider the temperature and the total pressure

$$P = p_{SO_2} + p_{H_2O} \qquad (2.13)$$

as control variables. The vapor pressure of water is given by

$$^{10}\log p_{H_2O} = 5.882 - 2198/T \qquad (2.14)$$

and then $[H^+]$ and $[HSO_3^-]$ may again be expressed in terms of $[SA^-]$ and of the control variables. In both cases, the delignification, the hemicellulose dissolution and the formation of strong acids are then uniquely determined by the control variables and by the initial state of the process.

3. MATHEMATICAL FRAMEWORK FOR THE OPTIMIZATION PROBLEM.

In this section we will briefly account for the mathematical concepts involved in the optimization problem. We will thus consider the acid sulfite cooking process as a dynamic system described by the following set of ordinary nonlinear differential equations.

$$\frac{dx}{dt} = f(x,u;t) \qquad x(t_0) = x_0 \tag{3.1}$$

where $x(t)$ is the n-dimensional state vector and $u(t)$ is the m-dimensional control vector. $x(t_0)$ is the initial state of the system. For the basic model given in Section 2, we then obviously have $n = 3$ (lignin, hemicellulose and strong acids) and $m = 2$ (temperature and pressure). However, it will later (Section 5) prove to be necessary to introduce further state variables, and thus the order of the system will increase.

Given the system (3.1), we then define the cost functional

$$J = F\left(x(t_f);t_f\right) + \int_{t_0}^{t_f} L(x,u;t)dt \tag{3.2}$$

where F is a function of the terminal state, that is the state at time t_f. The terminal time t_f is a priori fixed, and the time interval $[t_0,t_f]$ thus represents the length of the cooking time.

In general, it is necessary to put different kinds of restrictions on the class of control strategies that we consider. For example, for technological reasons the temperature and the pressure of the cook cannot be arbitrarily chosen. Thus, we also specify that the optimal solution

must satisfy the following set of constraints:

$$\begin{aligned} &\psi(x(t_f);t_f) = 0 \\ &S(x;t) \leq 0 \qquad \forall t\in[t_0,t_f] \\ &g(x,u;t) \leq 0 \qquad \forall t\in[t_0,t_f] \end{aligned} \tag{3.3}$$

ψ is an s-dimensional ($s \leq n$) nonlinear vector function of the terminal state, and with this kind of constraints it will be possible to handle the condition that the desired terminal lignin concentration is 2%. The mixed state-control variable constraint g is a p-dimensional nonlinear vector function. The components of g are explicit functions of at least one control variable u_i, but the explicit dependence on x is arbitrary. In the following, constraints of this type are included to handle different kinds of constraints on the temperature and the pressure. For example, we will consider the case where the control variables are bounded by maximum available temperature and pressure, that is,

$$g_i = u_i - u_{i_{max}} \leq 0 \tag{3.4}$$

The dimension p of g is arbitrary, but to guarantee compatibility of the constraints, it is generally necessary to restrict the number of active constraints. This problem is further discussed in [4], where also other kinds of regularity conditions are given. Finally, we may specify that the optimal state variables lie within some prescribed boundaries, and this is formulated as $S(x;t) \leq 0$, where S may be a nonlinear vector function. The difference between the constraints g and S is that S does not depend explicitly on the control variables, while g does. The separation of these types of constraints may seem to be nonessential. However, from a mathematical point of view, constraints of the type $S(x;t) \leq 0$ are

much more difficult to handle, and they are also much harder to solve numerically. It turns out to be necessary to include this kind of constraints when we consider constrained temperature and pressure change rates (Section 5). We then introduce dT/dt and dP/dt as new control variables and T and P as new state variables, and the upper bounds on the temperature and the pressure then have to be formulated as constraints of the type $S(x;t) \leq 0$.

We may now finally formulate the optimal control problem as follows: Given the dynamic system (3.1) and the cost functional (3.2), determine the optimal control strategies $u(t)$ subject to the constraints (3.3), so that the cost functional is minimized.

The numerical solution of optimal control problems is generally far from easy, and many different algorithms have been proposed (see e.g. [4] for references). The best choice between the different methods is probably not uniquely determined, but since we had previous computational experiences from methods based on the Differential Dynamic Programming technique, this approach was used to develop a computer program. The DDP technique is thoroughly described in [3], and the algorithm for the problem stated above is given in [4], where also different computational aspects are discussed.

4. OPTIMAL CONTROL OF MODEL I. UNCONSTRAINED CONTROL CHANGE RATES.

We will consider the case when the formation of strong acids is given by (2.6) and when the control change rates are unconstrained. In 4.1 the necessary mathematical preparations are given, i.e. a compact mathematical model of the form (3.1), the cost functional and the specifications of the constraints. We also illustrate the properties of the model, and account for different problems connected to the applicability of the computer program. During the computations, further problems appeared, and these are discussed in 4.2. In particular, it is shown that it is necessary to introduce new state variables, and that the cost functional has to be modified. In 4.3 the optimal solutions for various terminal times t_f are then given, and the effect of the different approximations that have been made is discussed.

4.1. Preparations.

4.1.1. A compact mathematical model.

To get a compact mathematical model of the process, we introduce the following state variables:

x_1 = lignin content [L] (gram per 100 g of uncooked wood)

x_2 = hemicellulose content [C] (gram per 100 g of uncooked wood)

x_3 = concentration of strong acids [SA^-] (moles per litre)

In principle, the control variables can be chosen as the temperature of the liquor and the total pressure in the

digester. However, from a numerical point of view, it turned out to be favourable to choose

$$u_1 = \exp(-1/T)$$

instead of T (where T is measured in degrees Kelvin) as one of the control variables. This will also simplify the mathematical model. The second control variable is chosen as

u_2 = total pressure P (bar),

but it should be pointed out that this control variable will later also be changed (Section 5). To simplify the notations, we also introduce some additional (or slack) variables. Thus, $\tilde{u}_2$ is defined as the partial pressure of the sulphur dioxide in the gas phase (p_{SO_2}). From (2.13) then follows that

$$\tilde{u}_2 = u_2 - p_{H_2O} \tag{4.1}$$

where p_{H_2O}, the partial pressure of water, is given by (2.14)

$$^{10}\log p_{H_2O} = 5.882 - 2198/T$$

Thus,

$$\tilde{u}_2(u) = u_2 - c_3 u_1^{c_4}$$

where

$$c_3 = 10^{5.882}$$

$$c_4 = 2198 \cdot {}^{e}\log 10$$

We also introduce x_3 as the concentration $[HSO_3^-]$ of hydrogen sulfite ions. From (2.10) and (2.11) follows that

$$[HSO_3^-] = ([Na^+]-[SA^-])/2 + \sqrt{([Na^+]-[SA^-])^2/4 + K_{p_{SO_2}} p_{SO_2}}$$

and thus

$$r = ([Na^+]-x_3)/2 + \sqrt{([Na^+]-x_3)^2/4 + \tilde{u}_2(u) K_{p_{SO_2}}} \qquad (4.2)$$

To further abbreviate the notations, we also set ℓ_{12} equal to the equilibrium constant $K_{p_{SO_2}}$, i.e.

$${}^{10}\log \ell_{12}(u) = - c_1 \, {}^{e}\log u_1 - c_2 \qquad (4.3)$$

where

$$c_1 = 2665$$

$$c_2 = 10.208$$

Since the concentration of sodium ions from the ionic medium is kept constant, we also define

$$N = [Na^+]$$

(Unless otherwise explicitly stated, the numerical value of N is equal to 0.375.) Substituting ℓ_{12} and N into (4.2) we get

$$r(x,u) = (N-x_3)/2 + \sqrt{(N-x_3)^2/4 + \tilde{u}_2(u)\ell_{12}(u)} \qquad (4.4)$$

and the rate equations (2.2), (2.3) and (2.6) then finally become:

$$\frac{dx_1}{dt} = f_1(x,u) = - k_1(x) u_1^{\ell_1(x)} x_1^{\ell_4(x)} [\, r(x,u)\,]^{\ell_5(x)-\ell_6(x)} \cdot$$

$$\cdot\, [\tilde{u}_2(u)\, \ell_{12}(u)\,]^{\ell_6(x)}$$

$$\frac{dx_2}{dt} = f_2(x,u) = - k_2 u_1^{\ell_2} x_2^{\ell_7} [\, r(x,u)\,]^{-\ell_8} [\tilde{u}_2(u)\, \ell_{12}(u)\,]^{\ell_8} \qquad (4.5)$$

$$\frac{dx_3}{dt} = f_3(x,u) = \begin{cases} - \dfrac{dx_1}{dt}\left\{\dfrac{x_3}{[L]_o - x_1} + k_4\left([L]_o - x_1\right)\right\} + \\ + k_3 u_1^{\ell_3} \left([L]_o - x_1\right)^{\ell_9} [\, r(x,u)\,]^{\ell_{10}-\ell_{11}} \cdot \\ \cdot\, [\tilde{u}_2(u)\, \ell_{12}(u)\,]^{\ell_{11}} \quad \text{if } x_1 < [L]_o \\ - k_5 \dfrac{dx_1}{dt} \quad \text{if } x_1 = [L]_o \end{cases}$$

The initial conditions are:

$$\begin{aligned} x_1(0) &= [L]_o = 28 \\ x_2(0) &= [C]_o = 32 \\ x_3(0) &= [SA^-]_o = 0.0 \end{aligned} \qquad (4.6)$$

The parameters k_1, ℓ_1, ℓ_4, ℓ_5 and ℓ_6 are functions of x_1, and the numerical values are:

$$k_1(x) = \begin{cases} k_1^H = 0.4845 \cdot 10^{16} & x_1 > x_1^B = 12.4 \\ k_1^L = 0.1464 \cdot 10^{16} & x_1 \leq x_1^B \end{cases} \quad (= k_L^o)$$

$$\ell_1(x) = \begin{cases} \ell_1^H = 12495 & x_1 > x_1^B \\ \ell_1^L = 12506 & x_1 \leq x_1^B \end{cases} \quad (= E_L)$$

$$\ell_4(x) = \begin{cases} \ell_4^H = 0.6463 & x_1 > x_1^B \\ \ell_4^L = 1.6212 & x_1 \leq x_1^B \end{cases} \quad (= m) \qquad (4.7)$$

$$\ell_5(x) = \begin{cases} \ell_5^H = 0.8186 & x_1 > x_1^B \\ \ell_5^L = 0.7646 & x_1 \leq x_1^B \end{cases} \quad (= \alpha)$$

$$\ell_6(x) = \begin{cases} \ell_6^H = 0.7053 & x_1 > x_1^B \\ \ell_6^L = 0.7794 & x_1 \leq x_1^B \end{cases} \quad (= \beta)$$

All other parameters are constant during the cook, and the numerical values are:

$$\begin{aligned} k_2 &= 0.4541 \cdot 10^{15} && (= k_C^o) \\ k_3 &= 0.2824 \cdot 10^{16}/4.5 && (= k_{SA}^o/v) \\ k_4 &= -\ 0.002584/4.5 && (= h/v) \\ k_5 &= 0.09703/4.5 && (= g/v) \\ \ell_2 &= 14031 && (= E_C) \\ \ell_3 &= 15715 && (= E_{SA}) \\ \ell_7 &= 2.5420 && (= h) \\ \ell_8 &= 0.7069 && (= \nu) \\ \ell_9 &= 2.3991 && (= s+1) \end{aligned} \qquad (4.8)$$

(Contd. p. 20)

$$\ell_{10} = 1.5287 \quad (= \delta)$$
$$\ell_{11} = 0,6903 \quad (= \varepsilon)$$
$$N = 0.3750 \quad (= [Na^+])$$

(4.8) (Contd.)

4.1.2. The cost functional and the constraints.

Given the dynamical system (4.5) with initial conditions (4.6), we may now formulate the following optimal control problem:

Determine $u(t)$, $0 \leq t \leq t_f$, such that

$$J = -x_2(t_f) \tag{4.9}$$

is minimized, i.e. such that $x_2(t_f)$ (final hemicellulose concentration) is maximized. (The terminal time t_f is fixed, but we will below investigate the role of t_f by computing the optimal strategies for some different terminal times.) The optimal control strategies must also satisfy the following constraints:

$$x_1(t_f) = x_1^{FIN} = 2.0$$

$$\left.\begin{aligned} u_1^{MIN} \leq u_1(t) \leq u_1^{MAX} \\ u_2^{MIN} \leq u_2(t) \leq u_2^{MAX} \end{aligned}\right\} \forall\, t \in [0,t_f] \tag{4.10}$$

The terminal constraint $(x_1(t_f) = 2.0)$ is due to the desired final lignin concentration, while the control variable constraints are due to technological constraints on the digester. The numerical values of the upper and lower control variable bounds are:

$u_1^{MIN} = \exp(-1/293)$

$u_1^{MAX} = \exp(-1/423)$

$u_2^{MIN} = 0.0$ (bar)

$u_2^{MAX} = 10.0$ (bar)

that is, the temperature T is bounded between $293^{o}K$ (room temperature) and $423^{o}K$.

4.1.3. Properties of the solutions of the system equations.

Inspection of the system equations (4.5) shows that x_1 and x_2 are decreasing for all t, u_1 and u_2, while x_3 is generally increasing. A typical control strategy is shown in Fig. 4.1 together with the corresponding trajectories. Simulations with different control strategies also show that u_1 and u_2 primarily affect the decreasing rates of x_1 and x_2, and that the decreasing rates are more sensitive with respect to changes in u_1 than in u_2.

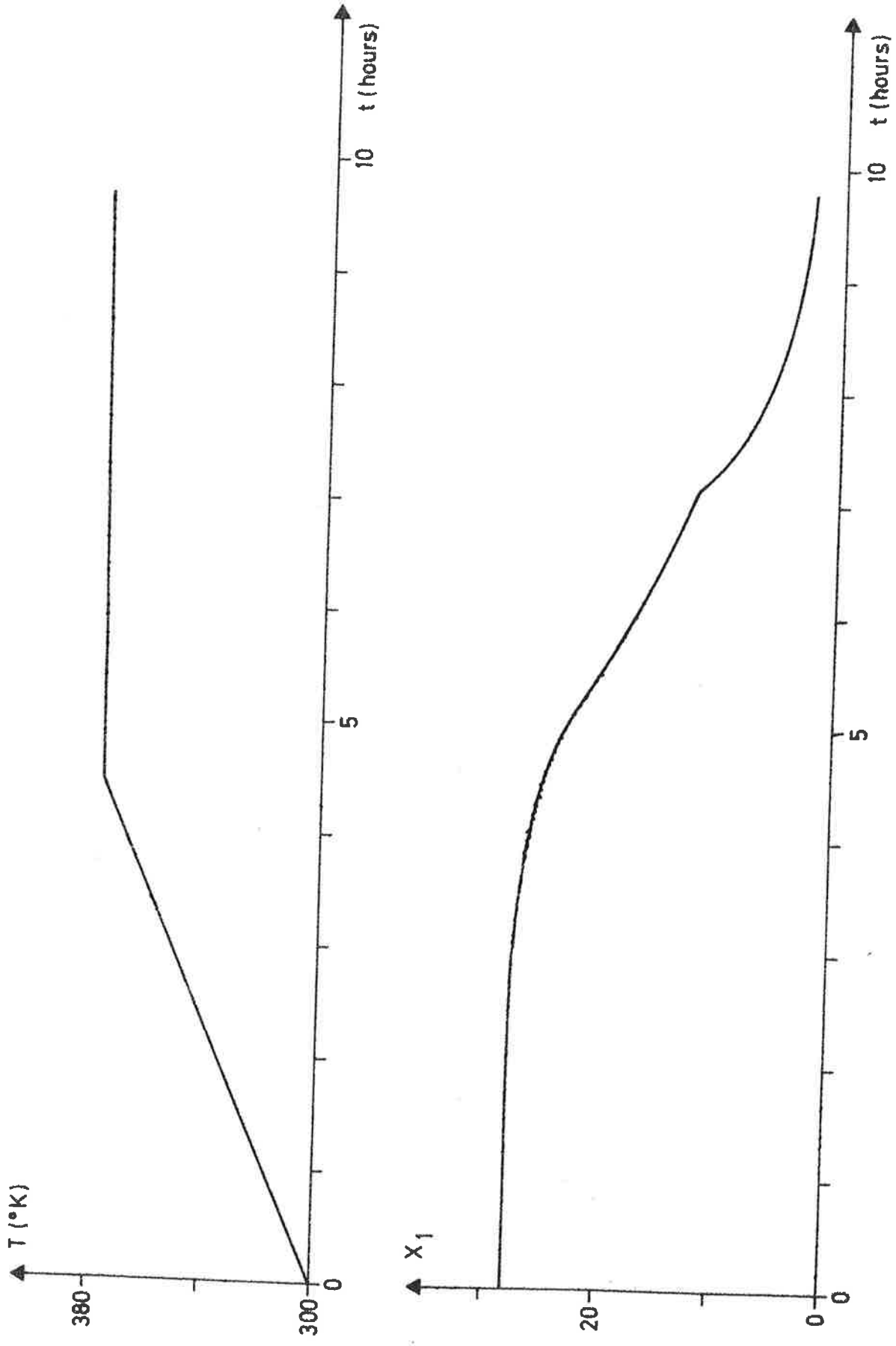

Fig. 4.1 - Solution of the system equations (4.5) for a typical control strategy. The pressure u_2 is raised from 1 bar to 10 bars in the same way as the temperature.

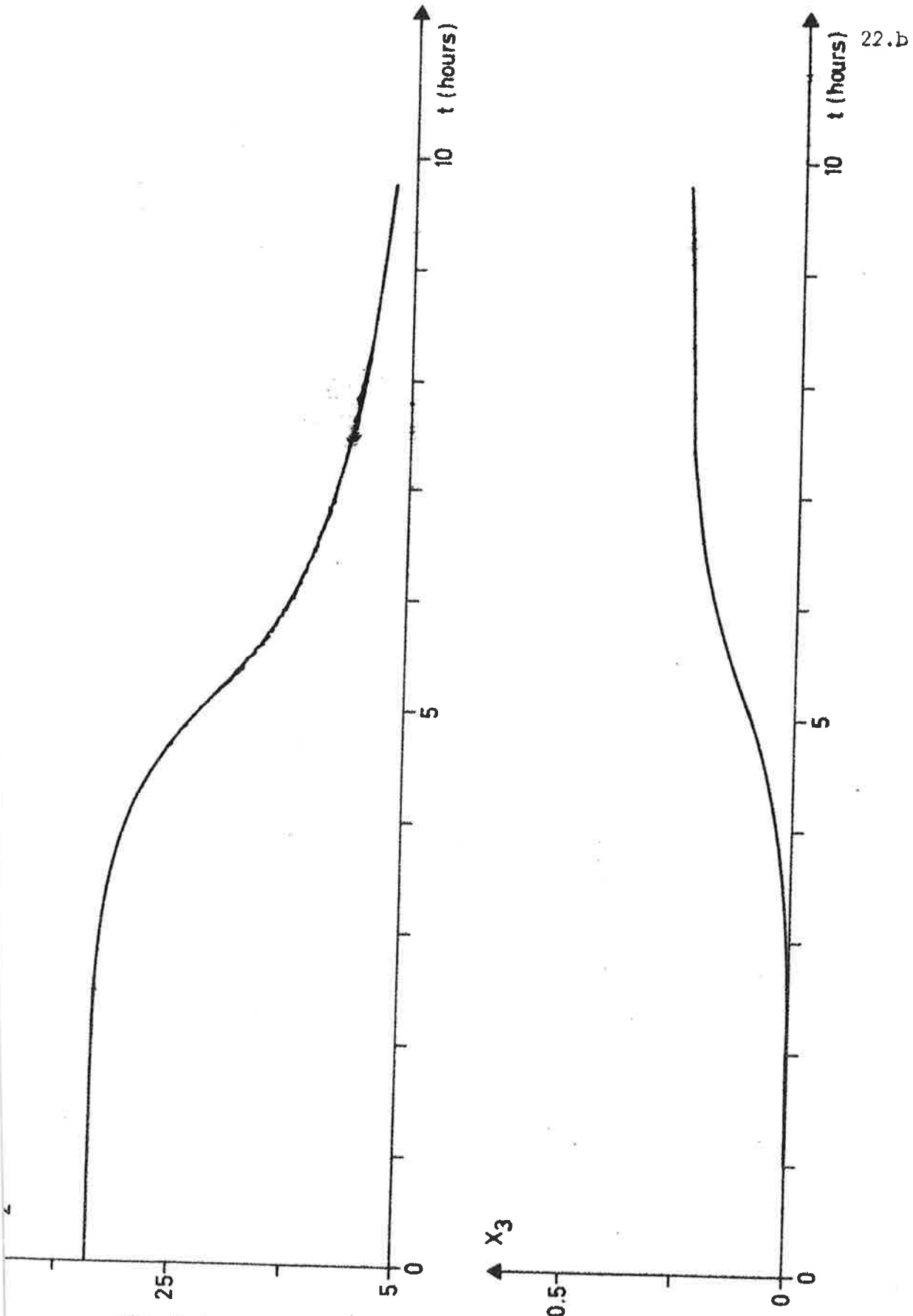

Fig. 4.1 - continued

4.1.4. Some consequences of the discontinuities of the system equations.

The system equations (4.5) have several non-desirable properties, such as complexity and discontinuous right-hand sides. In this section we will discuss the consequences of the discontinuities, and show that it is necessary to approximate them with smooth functions.

It can be shown [1], that discontinuities of the type (4.5) will produce discontinuities in the adjoint variables $\lambda(t)$, and the magnitude of these jumps are not a priori known. To solve the optimal control problem, we would thus have to include these jumps, and to handle them in the same way as the boundary conditions of the adjoint variables, i.e. to successively update the initial guess. However, this would considerably increase the complexity of the computer program, and it was thus decided to try to approximate the discontinuities with smooth functions. These functions should then have the properties that they generate an approximation of the discontinuities of $\lambda(t)$. Besides, the DDP algorithm requires that f is twice continuously differentiable with respect to both x and u, and a natural approximation then turns out to be:

$$k_1(x) = \frac{k_1^H + k_1^L}{2} + \frac{k_1^H - k_1^L}{\pi} \arctan[K(x_1 - x_1^B)] \qquad (4.11)$$

and analogously for ℓ_1, ℓ_4, ℓ_5 and ℓ_6 (4.7). We will refer to K as the smoothing parameter, and it is easily verified that the larger K is, the better is the approximation. The discontinuity obviously corresponds to $K = +\infty$.

In Figs. 4.2 and 4.3 the solutions of the system equations are shown for $K = +\infty$ (discontinuous right-hand sides),

K = 10 and K = 2. Although f_1 changes considerably, it can be seen that the approximations have very little influence on the solutions. It was thus concluded that K = 10 yields a sufficiently good approximation and that K = 2 may also be used if K = 10 should create numerical difficulties in the integration of the adjoint variables, that is, in the simulation of the jump in $\lambda(t)$.

4.1.5. Choice of numerical integration method and of integration step length.

From Fig. 4.1 it can be concluded that the system equations (4.5) are not stiff, i.e. they do not contain both very fast and very slow time constants. Hence, a straightforward integration scheme can be used, and in the following a fourth order Runge-Kutta scheme with fixed step-size has been used for the simulations as well as in the computation of the optimal control strategies.

Since the integration step length will directly influence the execution time of the computer program, it should be favourable to choose as large a step length as possible.

Thus, the system equations were solved with both the step length h = 0.12 hours and with h = 0.04. The relative differences between the two simulations were always less than 0.6% and hence the step size h = 0.12 (corresponding to 100 steps for a typical simulation) proved to be sufficiently small for the integration of the system equations.

However, the optimization algorithm also includes the backwards integration of the adjoint variables $V_x(t)$ and of the matrix $V_{xx}(t)$ [4], and it can be seen from [4], that these equations will become stiff if the smoothing parameter K is

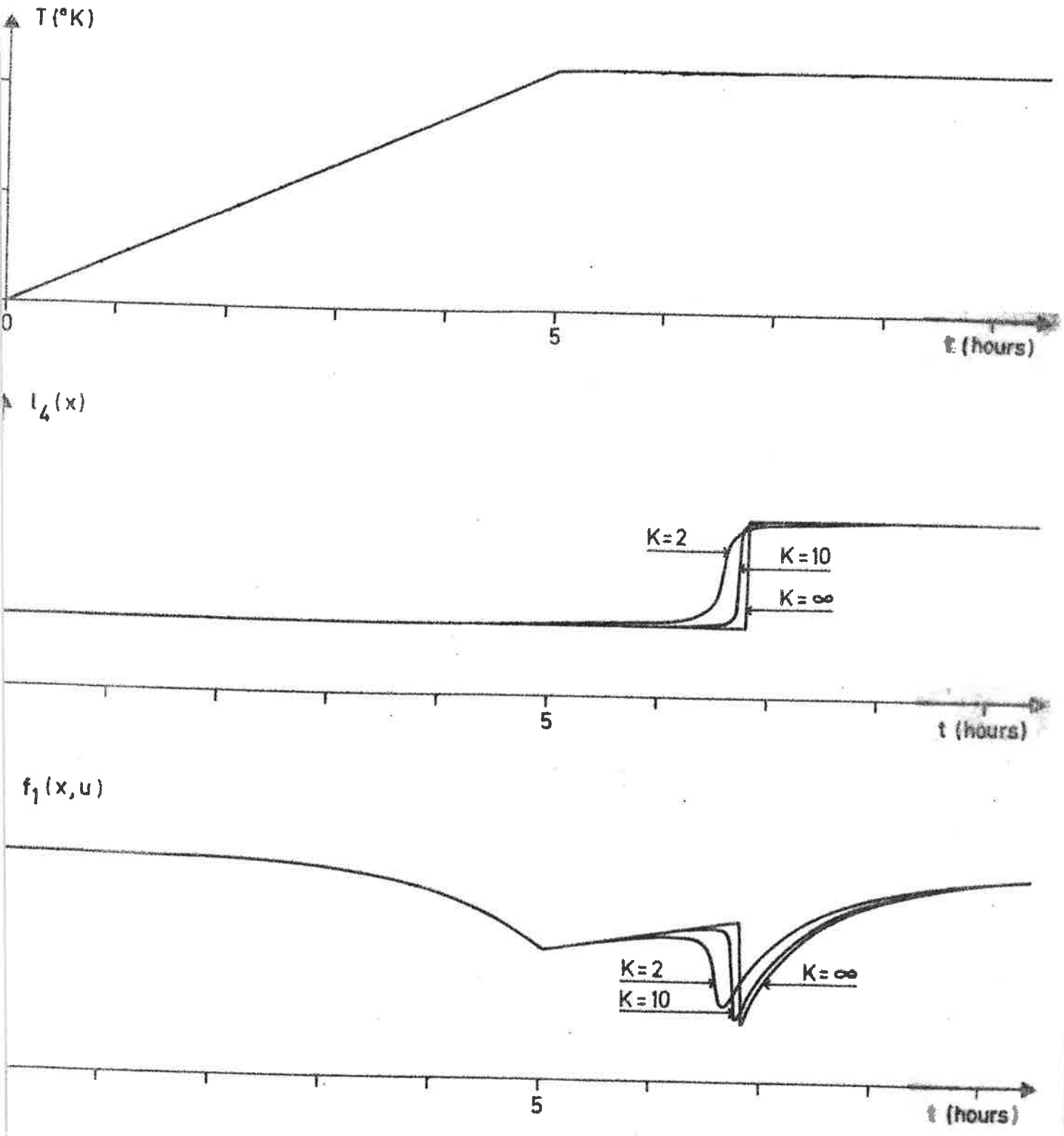

Fig. 4.2 - The parameter $\ell_4(x)$ and $f_1(x,u)$ for the smoothing parameters $K = +\infty$, $K = 10$ and $K = 2$. The same control strategy as in Fig. 4.1 was used.

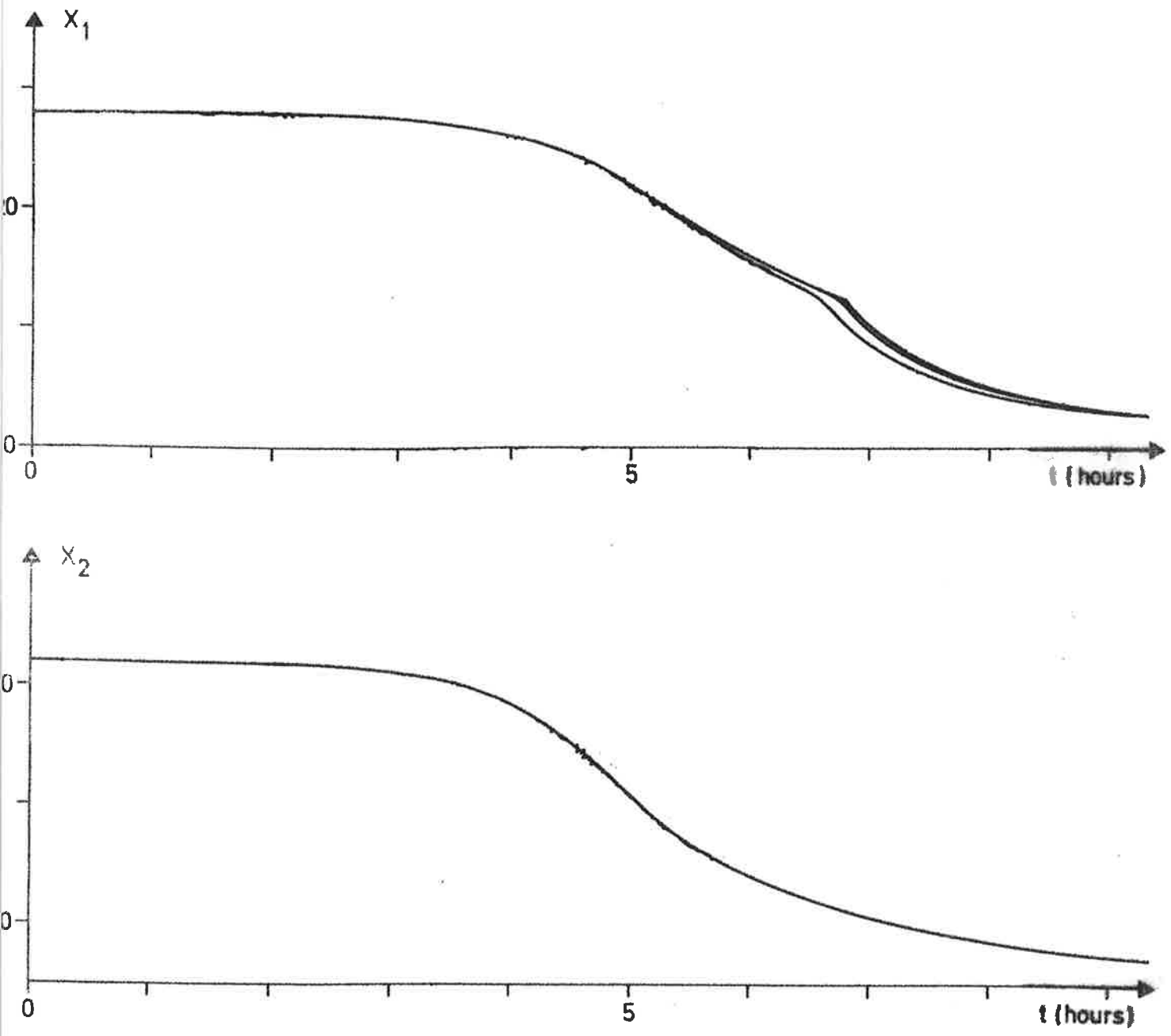

Fig. 4.3 - Corresponding solutions of the system equations.

large. Thus, if K is large and h is too large, the backwards integration will "explode" around $x_1 = x_1^B$. This is illustrated in Fig. 4.4. The full lines represent the optimal multipliers $V_x(t)$ for K = 10, computed with 500 integration steps. The dashed lines show the result when only 50 steps where used in the integration of $V_x(t)$. Obviously, there is a trade-off between the accuracy in the approximation of the discontinuities and the number of integration steps. Thus, 500 steps were required to avoid "explosion" for K = 10, while 100 steps was sufficient for K = 2. In the following, K = 2 and 100 steps has thus been used unless otherwise explicitly stated.

4.1.6. Minimization of the Hamiltonian.

In the DDP algorithm it is required that the Hamiltonian of the problem is minimized with respect to control variables. For the cost functional and the constraints given in Section 4.1.2, we thus have to minimize

$$H = V_{x_1} f_1 + V_{x_2} f_2 + V_{x_3} f_3 \tag{4.12}$$

subject to

$$g(u;t) = \begin{pmatrix} u_1 - u_1^{MAX} \\ -u_1 - u_1^{MIN} \\ u_2 - u_2^{MAX} \\ -u_2 - u_2^{MIN} \end{pmatrix} \leq 0 \tag{4.13}$$

for each t, $t \in [0, t_f]$. However, substituting the system equations (4.5) into (4.12), it is easily seen that an analytic minimization of H subject to the constraints

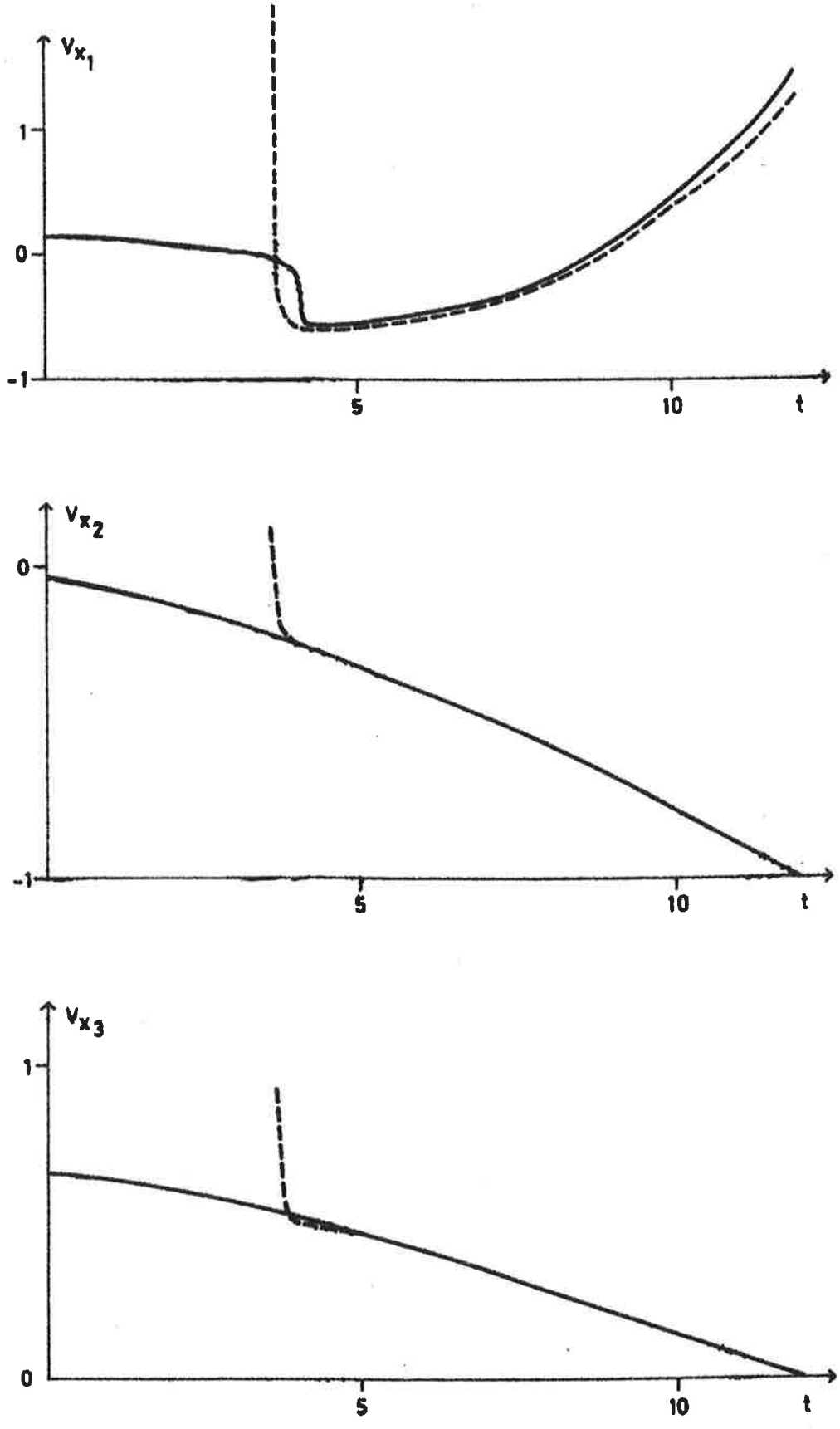

Fig. 4.4 - Computed optimal multipliers $V_x(t)$ for K = 10. Full lines correspond to 500 integration steps, dashed lines correspond to 50 steps. (The different step sizes give slightly different values of $x_1(t_f)$, which via the terminal constraint multiplier b affects the start value $V_{x_1}(t_f)$.)

(4.13) is very difficult or even impossible. It was thus necessary to carry out the minimization numerically, and a very simple search scheme was developed. First of all, the admissible region $g \leq 0$ was divided into a number of equally spaced points, and the numerical value of H for these points was determined. Then, the point where H attained its smallest value was chosen, and a new smaller search region was constructed around this point. This procedure was repeated until no further significant reduction of H could be obtained. In general, a search region consisting of 100 equally spaced points gave sufficient accuracy when repeated three times.

A distinct disadvantage of the method is that it is very time consuming. However, the method gave a very detailed insight into the structure of the Hamiltonian, and this proved to be very valuable. For example, in several cases it was possible to fix u_2 to its upper bound and then minimize only with respect to u_1. This is further illustrated below.

4.1.7. Modifications of the cost functional.

The cost functional as posed in Section 4.1.2 is

$$J = - x_2(t_f)$$

and the terminal constraint is

$$\psi = x_1(t_f) - 2.0 = 0 \qquad (4.14)$$

However, it turned out to be favourable to slightly modify J, and instead consider the cost functional

$$J = - x_2(t_f) + c\left(x_1(t_f) - 2.0\right)^2 \tag{4.15}$$

with the constraint (4.14). This may seem to be a meaningless modification, since the minimal values (and the optimal control strategies) are the same for the original cost functional as for (4.15). However, the reason for this modification is due to the way the algorithm is constructed. The algorithm works with the adjoined cost functional

$$\bar{J} = F\left(x(t_f);t_f\right) + \int_{t_0}^{t_f} L(x,u;t)dt + b^T\psi\left(x(t_f);t_f\right) \tag{4.16}$$

where the multipliers b have to be determined so that the optimal solution of (4.16) satisfies the condition $\psi = 0$. The algorithm can thus be separated into two different phases. First the adjoined cost functional is minimized for a fixed value of the multipliers b. If the optimal solution of $\bar{J}$ does not satisfy $\psi = 0$, b is changed by a small quantity δb, so that the optimal solution of $\bar{J}(b+\delta b)$ reduces the norm of ψ. However, to start up the algorithm, it is necessary to guess a value of the terminal multipliers b, and generally the only natural guess is $b = 0$. For the cost functional $\bar{J} = - x_2(t_f)$ it is then clear that the optimal solution is to choose u_1 and u_2 so small that no reaction takes place in the digester. From these nominal strategies (which are far away from the optimal ones) it turned out to be impossible to get successful changes in b, and the algorithm failed to converge. However, the modified cost functional (4.15) forces the control variables to act, since the additional term otherwise would contribute too much to the cost. Theoretically, the optimal solution of (4.15) can be forced to satisfy $\psi = 0$ by letting c tend to infinity. However, this would create new numerical problems, and thus $c = 1$ was chosen since this proved to be sufficient to make the algorithm converge.

4.1.8. Calculation of partial derivatives.

Since the algorithm is based on a second order Taylor series expansion of the Hamilton - Jacobi - Bellman equation [4], it is necessary to have analytic expressions for the first and second order partial derivatives of f_i (4.5) with respect to both x and u. It turned out to be necessary to provide 53 non-zero different analytic expressions for the derivatives involved, and since many of them are very complex it was more or less a principal problem to avoid errors. This problem had to be solved by checking the analytic expressions against numerical differentiation, which was included in the DDP program so that also punching errors could be detected and eliminated. In fact, some errors with a critical influence on the performance of the algorithm were discovered in this way.

4.2. Change of State Variables and Further Modifications of the Cost Functional.

4.2.1. Change of state variables.

A straightforward application of the DDP algorithm to the problem stated in the previous section proved for various reasons to be unsuccessful. One major problem was that the adjoint variables $V_x(t)$ had a tendency to explode as t approached zero. This problem could not be overcome by any of the modifications given above, but is in fact inherent in the problem, as can be seen from equation (2.6). Thus it was natural to consider (2.7) instead, that is

$$\frac{d}{dt}\left\{[SA^-]/([L]_o-[L])\right\} = \frac{h}{v} r_L + \frac{k_{SA}}{v}([L]_o-[L])^S[HSO_3^-]^\delta[H^+]^\varepsilon \quad (4.17)$$

with the boundary condition

$$\left\{[SA^-]/([L]_o-[L])\right\}_{t=t_0} = \frac{h}{v}\{r_L\}_{t=t_0}$$

We thus define the new state variables

$$z_1 = x_1$$
$$z_2 = x_2$$
$$z_3 = 1000x_3/([L]_o-x_1)$$

(The factor 1000 was introduced to get the state variables of approximately the same magnitude.) Substituting $x_1 = z_1$, $x_2 = z_2$ and $x_3 = z_3([L]_o-z_1)/1000$ into $f_1(x,u)$, $f_2(x,u)$, (4.4) and (4.17), we then get

$$\frac{dz_1}{dt} = \hat{f}_1(z,u)$$

$$\frac{dz_2}{dt} = \hat{f}_2(z,u) \qquad (4.18)$$

$$\frac{dz_3}{dt} = -1000\, k_4\hat{f}_1(z,u) + 1000\, k_3 u_1^{\ell_3}([L]_o-z_1)^{\ell_9-1} \cdot [r(z,u)]^{\ell_{10}-\ell_{11}}[\tilde{u}_2(u)\ell_{12}(u)]^{\ell_{11}}$$

The initial conditions for z_1 and z_2 are obviously the same as for x_1 and x_2, and to determine the boundary condition for z_3, we notice that

$$x_3 = \frac{z_3([L]_o-x_1)}{1000} \qquad (4.19)$$

Differentiating (4.19) for t = 0, we get

$$\frac{dx_3}{dt} = \frac{dz_3}{dt}\,\frac{([L]_o - x_1)}{1000} - \frac{dx_1}{dt}\,\frac{z_3}{1000} = -\frac{dx_1}{dt}\,\frac{z_3}{1000}$$

since $x_1(0) = [L]_o$. But for t = 0, $dx_3/dt = -k_4 f_1(x,u)$, and thus

$$-k_5 f_1(x,u) = -f_1(x,u)\,\frac{z_3(0)}{1000}$$

which, since $f_1 \neq 0$ for t = 0, implies that

$$z_3(0) = k_5 \cdot 1000$$

This redefinition of the state variables proved to be successful, and at least close to the optimal solution the explosion tendency of the adjoint variables was eliminated. However, it turned out that for other reasons there could be explosions in $V_x(t)$. This is illustrated below.

4.2.2. A sequence of cost functionals.

Although the redefinition of the state variables highly improved the situation around the optimal solution, another difficult problem remained, namely to get the algorithm to converge. This proved to be almost impossible, even after all the modifications given above. The reason for this obviously is the strong nonlinearity of the problem, that is the second order Taylor expansions [4] are valid only in a very small neighbourhood of the optimal solution.

A possibility to handle this difficulty proved to be to successively modify the cost functional and to solve a sequence of optimization problems. We thus introduce the new cost functional

$$J = - x_2(t_f) + (x_1(t_f)-2.0)^2 + \int_0^{t_f} [\varepsilon_1(u_1-a_1)^2 + \varepsilon_2(u_2-a_2)^2]dt \qquad (4.20)$$

where $\varepsilon_i (\geq 0)$ and a_i are constants that have to be specified. Obviously, the original problem corresponds to $\varepsilon_i = 0$. Now suppose that we minimize (4.20) for some parameters a_i and for a large value of the parameters ε_i. Then the optimal control variables will generally not differ so very much from a_1 and a_2, and thus $u_1(t) = a_1$ and $u_2(t) = a_2$ should be a good initial guess when the ε_i:s are large. When the optimal solution is found, the ε_i:s are decreased and the latest optimal solution is used as the initial guess for the new problem. Repeating this procedure, the successive optimal solutions will approach the optimal solution of the original problem, and finally the ε_i:s can be set equal to zero. However, it turned out to be important not to reduce the ε_i:s too fast, since the differences between the initial guesses and the optimal solution otherwise could become too large.

It was found that when ε_2 decreased, u_2 approached the upper bound u_2^{MAX}. To simplify the computations, u_2 was then fixed to its upper bound while ε_1 was successively reduced. Having computed the optimal control $u_1^*(t)$ for this problem, $u_1(t) = u_1^*(t)$ and $u_2(t) = u_2^{MAX}$ were used as the initial guess for the original problem, and it was found that it in fact was the optimal solution.

The importance of having sufficiently close initial guesses is illustrated in Figs. 4.5 and 4.6. u_2 is fixed to its upper bound and the parameters are: $\varepsilon_1 = 0.5$, $a_1 = 0.95$. The full lines show the optimal solution of (4.20). The dashed lines in Fig. 4.5 correspond to the initial guess $u_1(t) = 0.98$ and to the adjoint variables $V_{z_i}(t)$ in the first iteration. The dotted lines correspond to $u_1(t)$ after one iteration and to the adjoint variables in the second iteration. As can be seen, $V_{z_i}(t)$ explode as t approaches zero, and thus it was impossible to reach the optimal solution with this particular initial guess. In Fig. 4.6 the optimal control for $\varepsilon = 2.0$ (dotted line) is used as the initial guess for $\varepsilon = 0.7$. The optimal solution then corresponds to the dashed line. With this as the initial guess for $\varepsilon = 0.5$, the optimal solution (full line) was found without any convergence problems.

The convergence problems are due to many facts. In particular, it was found that J was a very flat functional in the neighbourhood of the optimal solution. This is illustrated in Fig. 4.7. The full line is the optimal solution for $t_f = 12.0$, and the corresponding cost is $J = -11.36$. The dashed line, although considerably different from the optimal solution, yields $J = -11.35$.

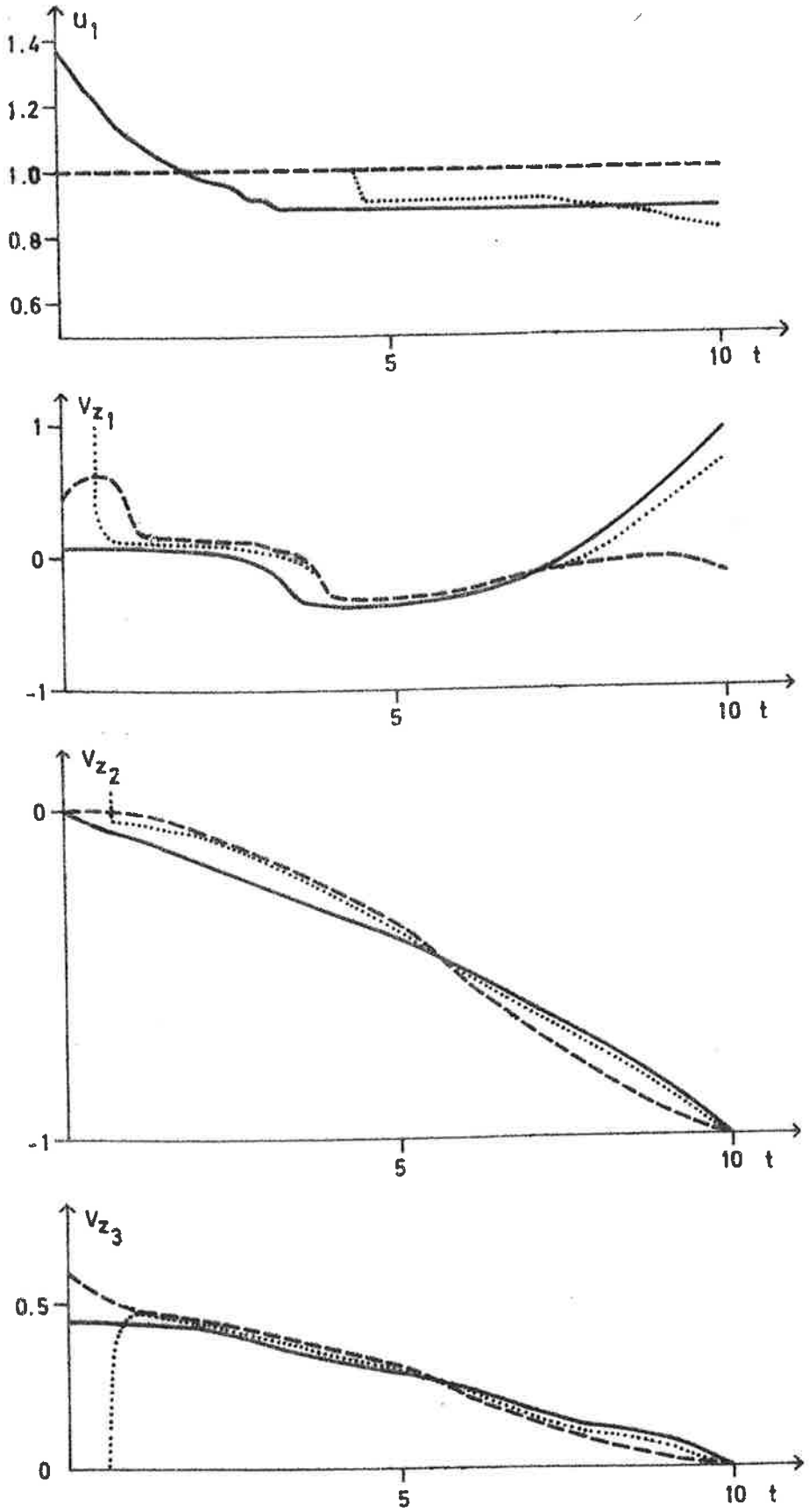

Fig. 4.5 - Convergence problems for $\varepsilon = 0.5$. Full line - optimal solution for $\varepsilon = 0.5$, dashed line - initial guess of $u_1(t)$ and adjoint variables in the first iteration, dotted line - $u_1(t)$ after one iteration and adjoint variables in the second iteration.

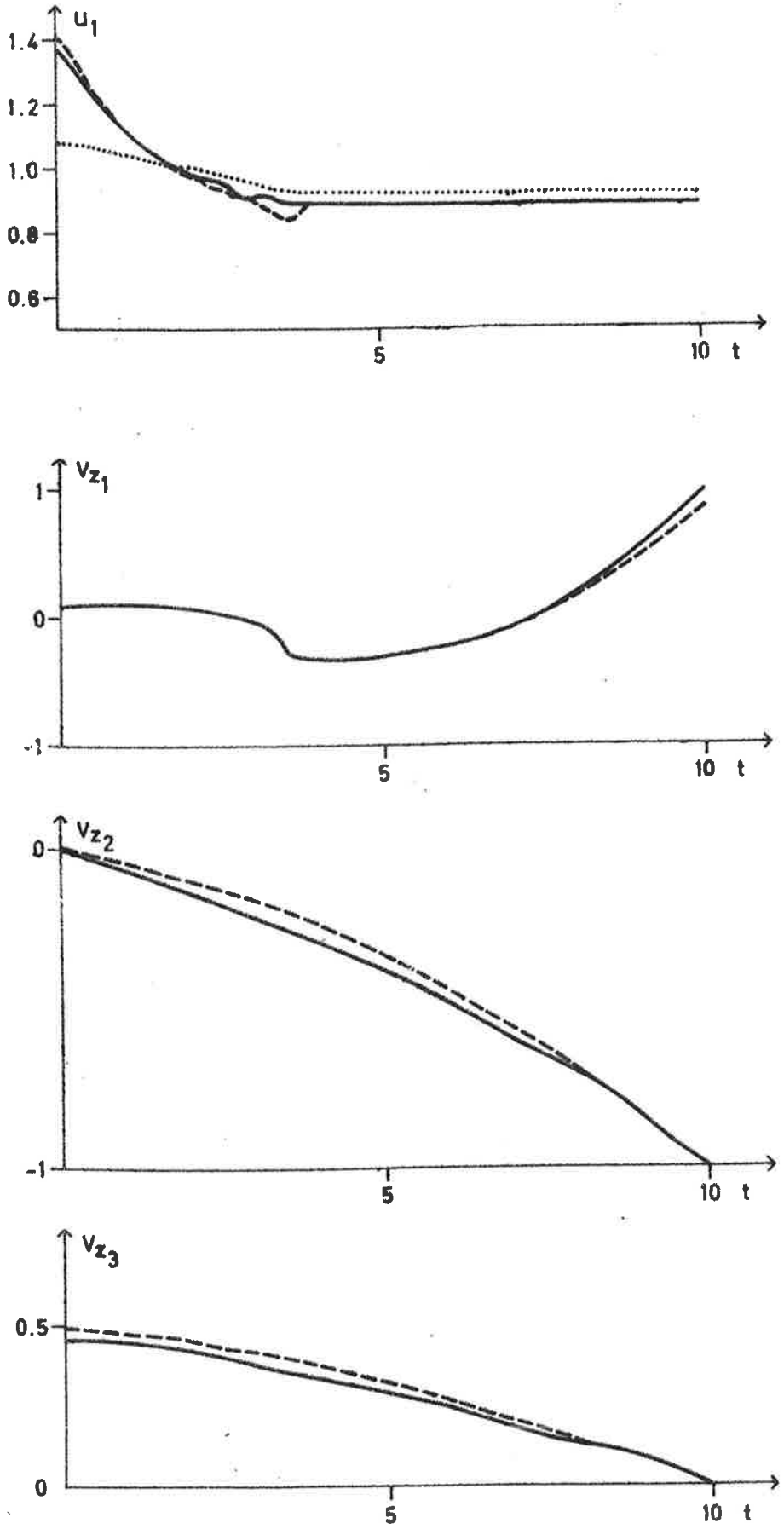

Fig. 4.6 - Successive optimal solutions for $\varepsilon = 2.0$ (dotted line), $\varepsilon = 0.7$ (dashed lines), and $\varepsilon = 0.5$ (full lines).

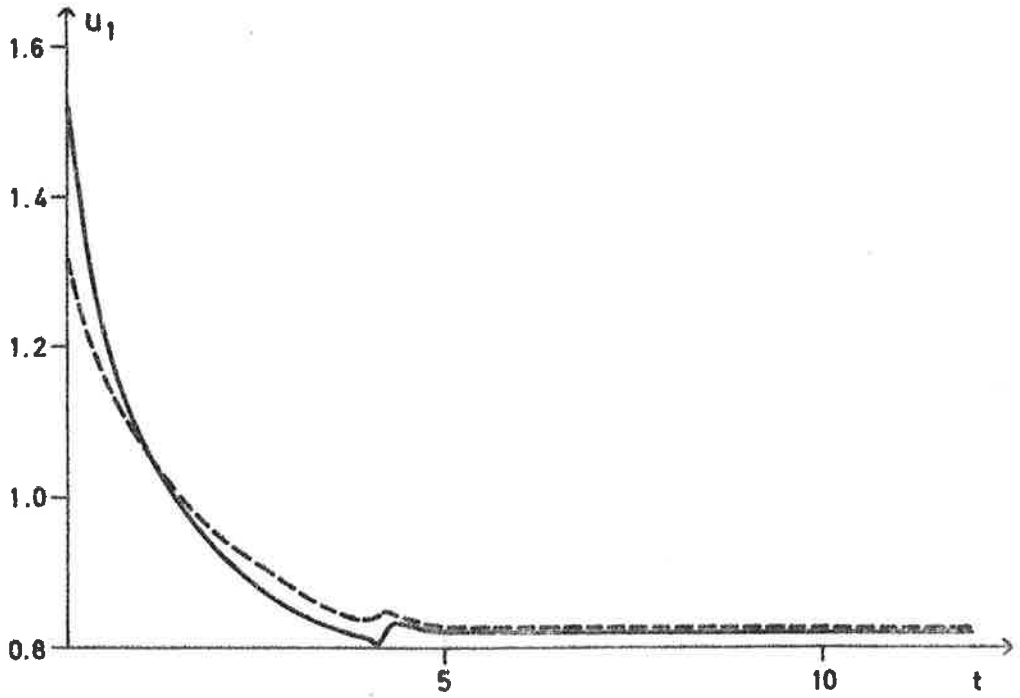

Fig. 4.7 - Illustration of the insensitivity of J around the optimal solution. Full line (optimal control) yields J = -11.36 while dashed line yields J = -11.35.

4.3. Optimal Solutions.

4.3.1. Optimal solutions for various terminal times.

Applying the modifications and the techniques described in the previous sections, the optimal solutions for the problem could finally be determined. It then turned out that the optimal control $u_2(t)$ attained its upper bound u_2^{MAX} (= 10 bars) over the whole time interval $[0,t_f]$. The computed optimal temperature strategy is shown in Figs. 4.8 and 4.9 for the terminal times t_f = 12, 10, 8 and 6 hours. Notice, that T is determined by $u_1(t) = \exp(-1/T)$. The corresponding optimal trajectories $z_1(t)$ (lignin) and $z_2(t)$ (hemicellulose) are also shown.

In Fig. 4.10, the maximum hemicellulose yields $z_2(t_f)$ is given as a function of the cooking time t_f. This function should allow for a rational trade-off between the cooking time and the outcome of the process. The point A represents the hemicellulose content when the control strategy in Fig. 4.1 is applied to the process.

4.3.2. The influence of the discontinuity approximation.

The optimal solutions shown in Figs. 4.8 and 4.9 were computed with the smoothing parameter K = 2 (4.11). It is thus natural to ask if this approximation had a crucial influence on the computed solutions, and if for example K = 10 would result in a considerably different optimal solution.

To investigate the influence of K, we have thus computed the optimal solution for K = 10 (using 500 integration steps), and the solutions for K = 10 and K = 2 are shown in Fig. 4.11. The full lines represent the optimal control

for K = 10 and the corresponding lignin and hemicellulose trajectories. The dashed line represents the optimal temperature strategy for K = 2, and it can be seen that it is very close to the solution for K = 10. In fact, no considerable difference can be noticed in the corresponding lignin and hemicellulose trajectories, and it was thus concluded that K = 2 was accurate enough.

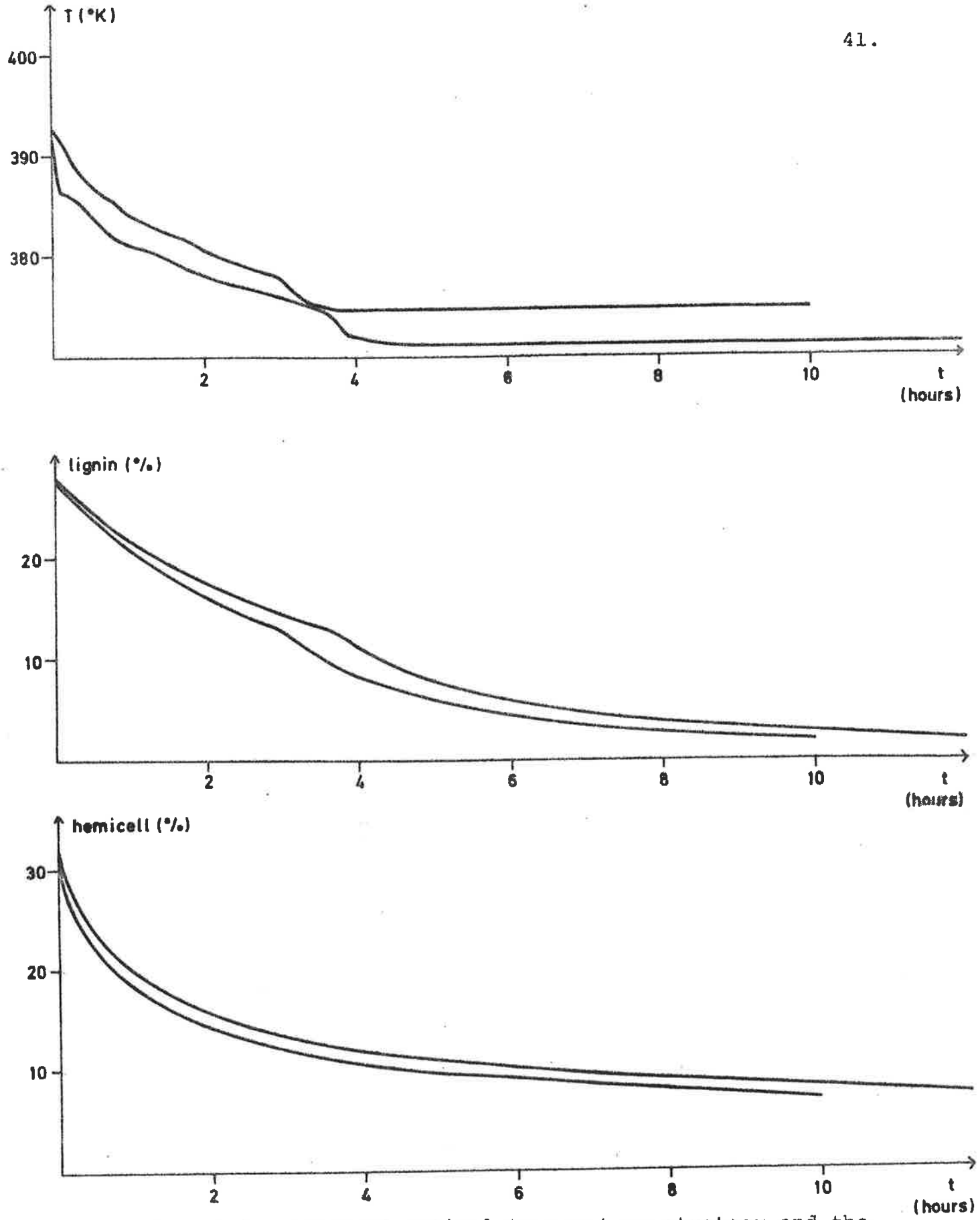

Fig. 4.8 - Computed optimal temperature strategy and the corresponding lignin and hemicellulose trajectories for t_f = 12 and t_f = 10 hours. The optimal pressure strategy i: $u_2(t)$ = const. = 10 bars.

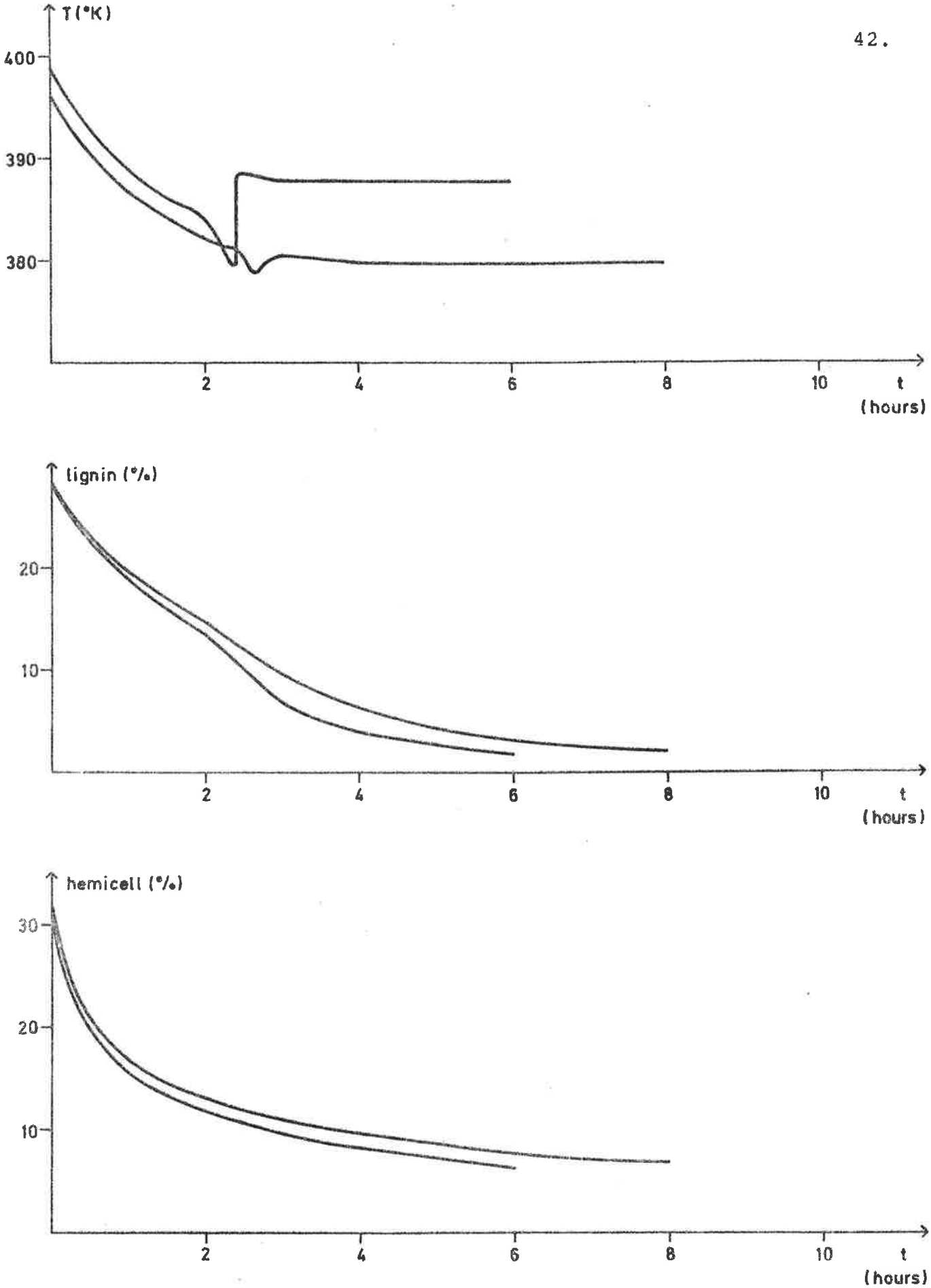

Fig. 4.9 - Optimal solutions for t_f = 8 and t_f = 6 hours.

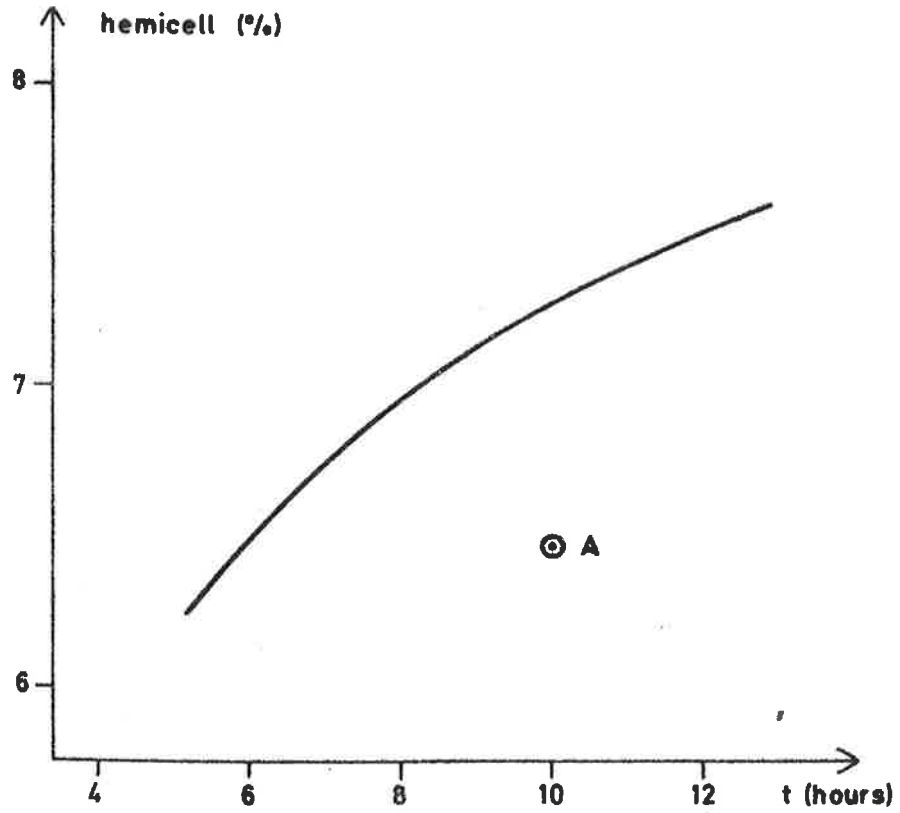

Fig. 4.10 - Optimal hemicellulose yield as a function of the cooking time t_f. The point A represents the yield for the strategy given in Fig. 4.1.

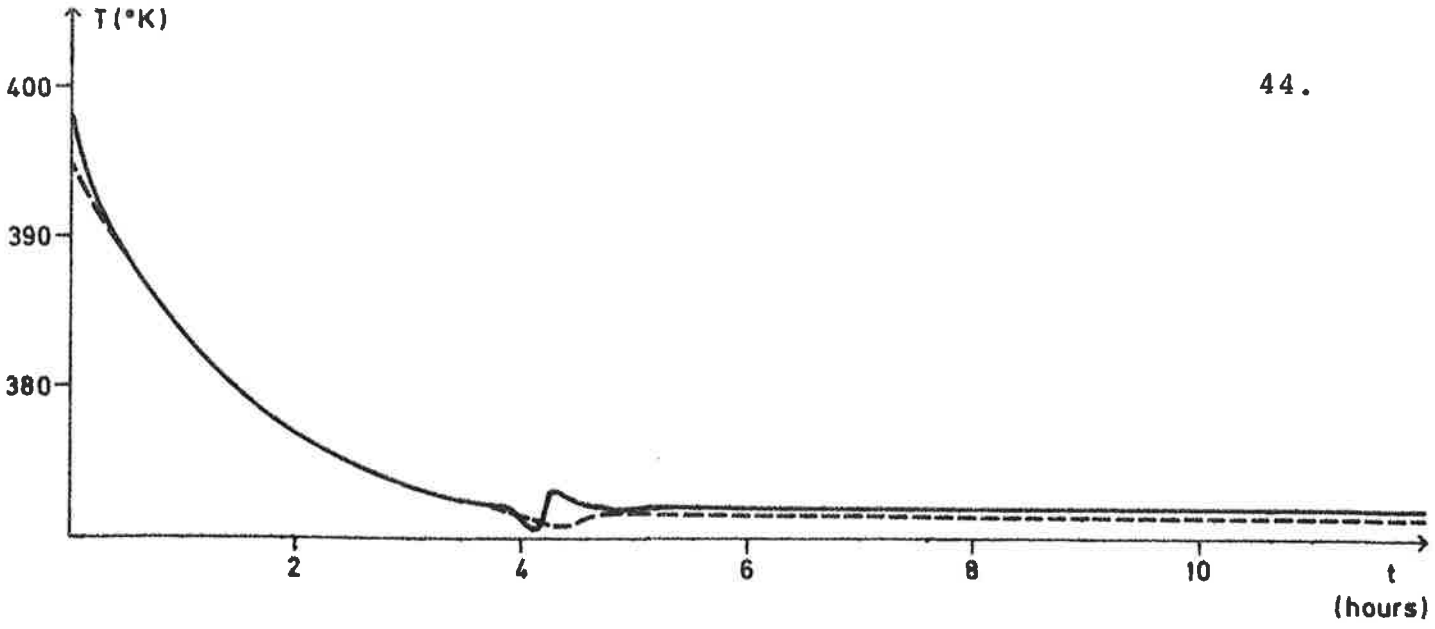

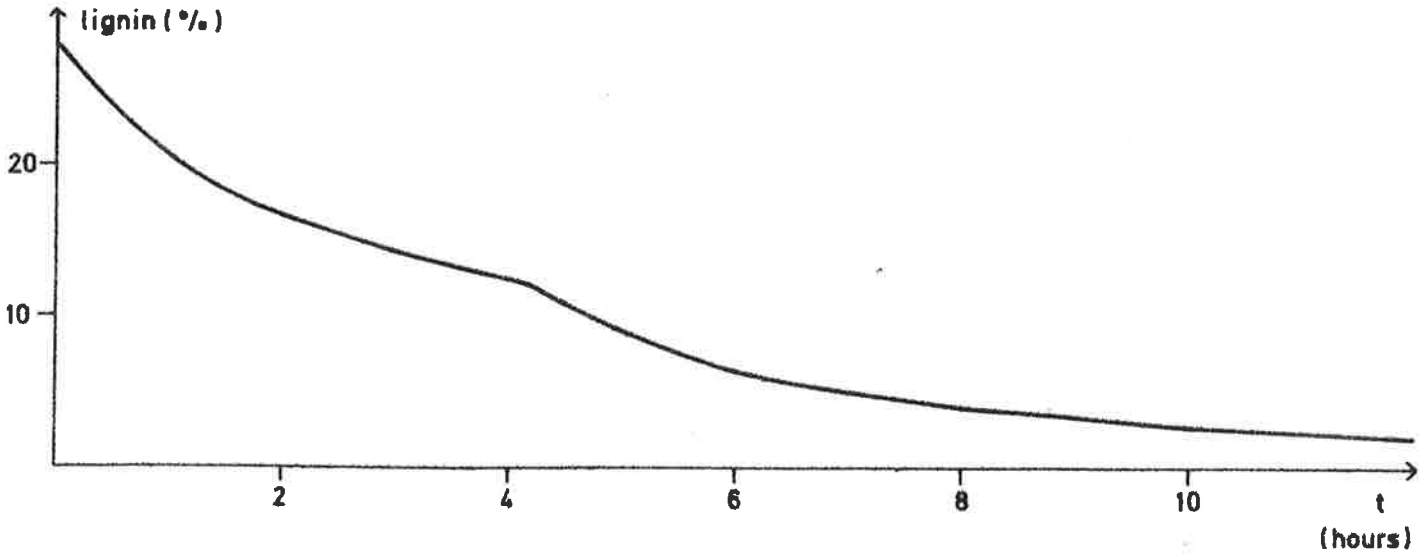

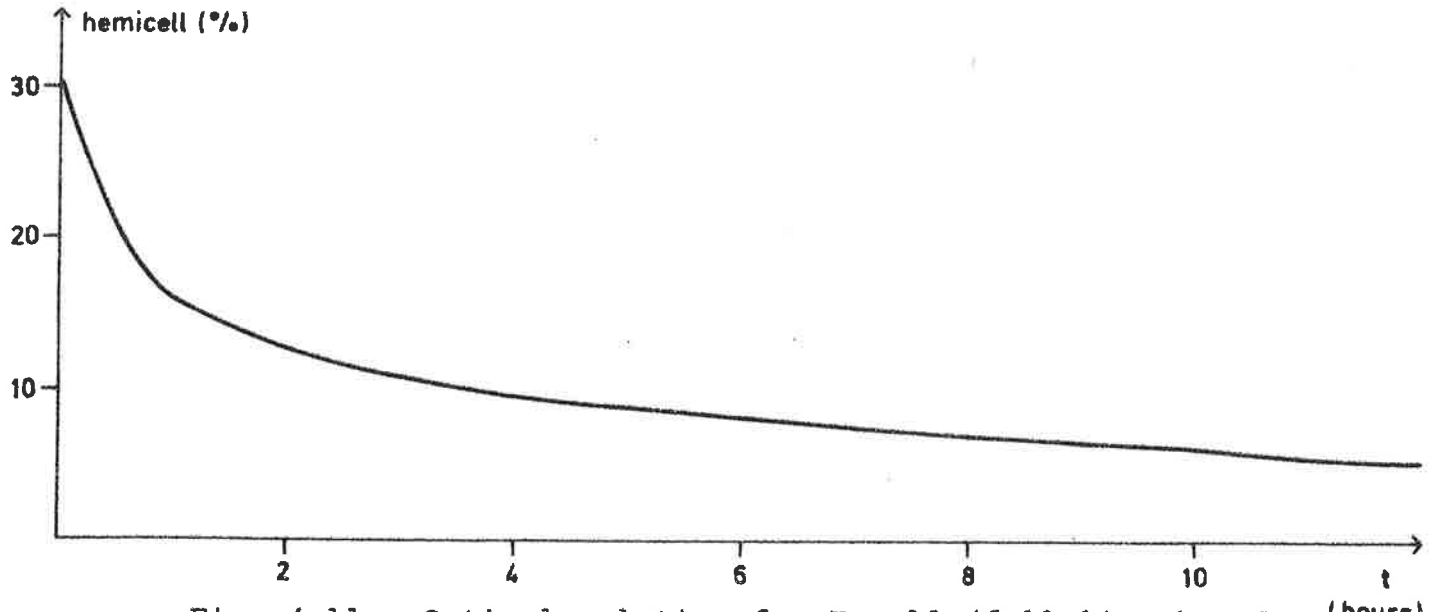

Fig. 4.11 - Optimal solution for K = 10 (full lines) and K = 2 (dashed line). The corresponding curves for lignin and hemicellulose coincide.

5. OPTIMAL CONTROL OF MODEL I. CONSTRAINED CONTROL CHANGE RATES.

In the previous section we tacitly neglected the fact that there in practice are further constraints on the control variables. Thus, it is not likely that the temperature and the pressure can be changed instantaneously from room temperature and room pressure to the optimal temperature and pressure at $t = 0$. In this section we will include these constraints in the problem. We will also consider the possibility to decrease the temperature of the process at the terminal time t_f, since this in practice is considered as a possibility to improve the quality of the pulp.

The introduction of the new constraints makes it necessary to redefine the state and the control variables of the process. Thus, in Section 5.1 we reformulate the problem, define the state and the control variables, give the new mathematical model and specify the constraints and the cost functional. It then turns out that our new problem is a singular problem with state variable constraints, and we briefly discuss the available solution methods for this class of problems. In Section 5.2 the computed optimal solutions are given.

5.1. Preparations.

5.1.1. A new mathematical model.

Since the temperature and pressure change rates now will be constrained, it is necessary to redefine the state and the control variables to be able to apply the optimal control theory outlined in Section 3. We thus introduce

$$u_1(t) = \frac{d}{dt}(T)$$

and

$$u_2(t) = \frac{d}{dt} p_{SO_2}$$

Notice that u_2 is chosen as the time derivative of the partial pressure p_{SO_2} and not as the time derivative of the total pressure P. The reason for this is that the total pressure is in practice controlled by the partial pressure of the sulphur dioxide, and the change rate of p_{SO_2} is for technological reasons constrained.

The state variables are defined as follows (compare Section 4.1):

$$\begin{aligned}
x_1 &= [L] && (\%) \\
x_2 &= [C] && (\%) \\
x_3 &= [SA^-]/([L]_o-[L])*1000 && ([SA^-] \text{ in moles/litre}) \\
x_4 &= 10^4 \cdot \exp(-3500/T) && (T \text{ in } {}^oK) \\
x_5 &= p_{SO_2} && (\text{bar})
\end{aligned} \qquad (5.1)$$

To abbreviate the notations, we also define

$$\ell_{12}(x) = K_{p_{SO_2}}(T)$$

$$\begin{aligned}
r_1(x) = [HSO_3^-] &= ([Na^+]-[SA^-])/2 + \\
&+\sqrt{([Na^+]-[SA^-])^2/4 + K_{p_{SO_2}} p_{SO_2}} = \\
&= \left(N - x_3([L]_o-x_1)\right)/2 + \\
&+\sqrt{\left(N - 0.001x_3([L]_o-x_1)\right)^2/4 + x_5\ell_{12}(x)}
\end{aligned}$$

$$r_2(x) = [H^+] = K_{p_{SO_2}} p_{SO_2} / [HSO_3^-] = x_5 \ell_{12}(x) / r_1(x)$$

The system equations then are

$$\frac{dx_1}{dt} = f_1(x,u) = - k_1(x) x_4^{\ell_1(x)} x_1^{\ell_4(x)} [r_1(x)]^{\ell_5(x)} \cdot [r_2(x)]^{\ell_6(x)}$$

$$\frac{dx_2}{dt} = f_2(x,u) = - k_2 x_4^{\ell_2} x_2^{\ell_7} [r_2(x)]^{\ell_8} \qquad (5.2)$$

$$\frac{dx_3}{dt} = f_3(x,u) = - k_4 f_1(x,u) + k_3 x_4^{\ell_3} ([L]_o - x_1)^{\ell_9 - 1} \cdot [r_1(x)]^{\ell_{10}} [r_2(x)]^{\ell_{11}}$$

$$\frac{dx_4}{dt} = f_4(x,u) = x_4 [{}^e\log(10^4/x_4)]^2 u_1/3500$$

$$\frac{dx_5}{dt} = f_5(x,u) = u_2$$

The initial conditions are:

$$\begin{aligned} x_1(0) &= 28. && (= [L]_o) \\ x_2(0) &= 32. \\ x_3(0) &= k_5 \\ x_4(0) &= 10^4 \exp(-3500/293) && (T(0) = 293^oK) \\ x_5(0) &= 0 \end{aligned} \qquad (5.3)$$

As before, the parameters k_1, ℓ_1, ℓ_4, ℓ_5 and ℓ_6 are functions of x_1, but some of the numerical values differ from those in Section 4. Thus

$$k_1(x) = \begin{cases} k_1^H = 0.4845 \cdot 10^{(16-4\cdot 12495/3500)} & x_1 > x_1^B = 12.42 \\ k_1^L = 0.1464 \cdot 10^{(16-4\cdot 12506/3500)} & x_1 \leq x_1^B \end{cases}$$

$$\ell_1(x) = \begin{cases} \ell_1^H = 12495/3500 & x_1 > x_1^B \\ \ell_1^L = 12506/3500 & x_1 \leq x_1^B \end{cases}$$

$$\ell_4(x) = \begin{cases} \ell_4^H = 0.6463 & x_1 > x_1^B \\ \ell_4^L = 1.6212 & x_1 \leq x_1^B \end{cases}$$

$$\ell_5(x) = \begin{cases} \ell_5^H = 0.8186 & x_1 > x_1^B \\ \ell_5^L = 0.7646 & x_1 \leq x_1^B \end{cases}$$

$$\ell_6(x) = \begin{cases} \ell_6^H = 0.7053 & x_1 > x_1^B \\ \ell_6^L = 0.7794 & x_1 \leq x_1^B \end{cases}$$

The numerical values of the other parameters are (compare 4.8):

$$k_2 = 0.4541 \cdot 10^{(15-4\cdot 14031/3500)}$$

$$k_3 = (0.2824/v) \cdot 10^{(19-4\cdot 15715/3500)}$$

$$k_4 = -2.584/v$$

$$k_5 = 97.03/v \qquad (5.5)$$

(Contd. p.49)

ℓ_2 = 14031/3500 (5.5) (Contd.)

ℓ_3 = 15715/3500

ℓ_7 = 2.5420

ℓ_8 = 0.7069

ℓ_9 = 2.3991

ℓ_{10} = 1.5287

ℓ_{11} = 0.6903

N = 0.3750

v = 4.5

The equilibrium constant $K_{pSO_2}(T)$ is given by

$$^{10}\log K_{p_{SO_2}}(T) = 2665/T - 10.208$$

and thus

$$^{10}\log \ell_{12}(x) = c_1 + c_2\,{}^{e}\log x_4 \qquad (5.6)$$

where

$$c_1 = (4 \cdot 2665/3500)\,{}^{e}\log 10 - 10.208$$

and

$$c_2 = -2665/3500$$

5.1.2. The cost functional and the constraints.

The cost functional is the same as in Section 4.1, i.e.

$$J = - x_2(t_f)$$

where t_f is the à priori fixed terminal time. The terminal constraint

$$\psi(x(t_f)) = x_1(t_f) - 2.0 = 0 \tag{5.7}$$

is also unchanged, and for the reasons given above, we will thus consider the modified cost functional

$$J = - k_a x_2(t_f) + k_b (x_1(t_f) - 2.0)^2 \tag{5.8}$$

where the parameters k_a and k_b have been introduced to increase the flexibility of J. However, the control variables are not the same as in Section 4, and thus we get a new set of control variable constraints. Formally, they are the same as (4.10), i.e.

$$\left.\begin{aligned} u_1^{MIN} \leq u_1(t) \leq u_1^{MAX} \\ u_2^{MIN} \leq u_2(t) \leq u_2^{MAX} \end{aligned}\right\} \forall\ t \in [0, t_f] \tag{5.9}$$

but the numerical values of u_i^{MIN} and u_i^{MAX}, i.e. the upper and lower bounds of the possible temperature and pressure change rates, are not the same. We thus assume that

$$\begin{aligned} u_1^{MIN} &= - 40.0 && \text{(degrees Kelvin/hour)} \\ u_1^{MAX} &= 40.0 && \text{(degrees Kelvin/hour)} \\ u_2^{MIN} &= - 100.0 && \text{(bars/hour)} \\ u_2^{MAX} &= 7.0 && \text{(bars/hour)} \end{aligned} \tag{5.10}$$

Finally, we must also consider the fact that the temperature and the pressure are bounded. From the definition (5.1) of the state variables then follows that we will now also have constraints of the type $S(x;t) \leq 0$. Thus

$$P^{MIN} \leq p_{H_2O} + x_5(t) \leq P^{MAX}$$

and

$$T^{MIN} \leq -3500[{}^{e}\log(10^{-4}x_4)]^{-1} \leq T^{MAX}$$

where P^{MIN}, P^{MAX}, T^{MIN} and T^{MAX} are given in 4.1.2. However, it turns out that the temperature constraints will never be active (compare Section 4) and also that the pressure never tends to decrease below P^{MIN}. Thus, the only constraint we have to consider is

$$p_{H_2O} + x_5(t) \leq P^{MAX} \tag{5.11}$$

where p_{H_2O}, the partial pressure of water, is given by

$${}^{10}\log p_{H_2O} = 5.882 - 2198/T$$

Expressing T as a function of x_4, we then finally get the state variable constraint

$$S(x;t) = x_5 + d_1 x_4^{d_2} - P^{MAX} \leq 0 \tag{5.12}$$

where

$$d_1 = 10^{(5.882-4d_2)}$$

and

$$d_2 = 2198 \cdot {}^{e}\log 10/3500$$

5.1.3. Computational methods for singular problems.

Since the system equations (5.2) are linear in the control variables, the optimal solution either has singular subarcs or is of bang-bang character. However, for physical reasons the bang-bang character is very unlikely (compare Section 4), and to compute the numerical solution it is thus necessary to be able to handle the singular subarcs.

The characteristic property of singular problems is that the condition $H_u = 0$ does not determine the optimal control variables. Besides, in this case we have $H_{uu} = 0$, and thus the second order DDP algorithm referred to in Section 3 is not directly applicable. Different methods to overcome these difficulties by limit methods have been suggested [2]. The basic idea of these methods is to solve a sequence of regular problems whose solutions tend to the solution of the singular problem. In this section we will briefly outline a method given in [2], and it is also shown how this method was modified to improve the convergence rate close to the optimal solution.

A. ε-$\alpha(\cdot)$ algorithm.

In the ε-$\alpha(\cdot)$ algorithm, the cost functional of the original problem is modified through addition of the quadratic term

$$\int_0^{t_f} \Sigma\varepsilon_i \left(u_i(t) - \alpha_i(t)\right)^2 dt$$

where the functions $\alpha_i(t)$ and the parameters ε_i have to be chosen as follows:

(i) Set $\varepsilon_i = \varepsilon_i^k > 0$ and guess an initial nominal solution $\bar{u}_i(t)$, $t \in [0,t_f]$, $i = 1,\ldots,m$. Set $\alpha_i(t) = \bar{u}_i(t)$, $i = 1,\ldots,m$.

(ii) Minimize $J(\varepsilon^k)$ and let $u_i^k(t)$, $i = 1,\ldots,m$, be the minimizing control strategy.

(iii) Choose ε_i^{k+1} such that $0 < \varepsilon_i^{k+1} < \varepsilon_i^k$ and set $\bar{u}_i(t) = \alpha_i(t) = u_i^k(t)$, $i = 1,\ldots,m$. Return to (ii).

Generally, numerical instability occurs when the ε_i:s tend to zero, that is when the optimal solution of $J(\varepsilon^k)$ tends to the optimal solution of the singular problem. However, it was proved in [2] that the algorithm under suitable assumptions about the problem converges to the optimal solution even for fixed values of the parameters ε_i. In that case, the magnitude of the ε_i:s will determine the convergence rate, and the smaller the ε_i:s are, the faster will the algorithm converge.

B. Modified ε-$\alpha(\cdot)$ algorithm.

The modification of the cost functional and the initial choice of the functions $\alpha_i(t)$ are the same as above. However, we now keep ε_i fixed and minimize $J(\varepsilon)$ with the second order DDP algorithm. After each successful iteration we then change the functions $\alpha_i(t)$, so that $\alpha_i(t) = u_i(t)$, $i = 1,\ldots,n$, where $u_i(t)$ is the new no-

minal control variables. This modification proved to increase the convergence rate close to the optimal singular solution, and was thus used when an approximative solution had been obtained with the ε-$\alpha(\cdot)$ algorithm.

5.1.4. Computational method for the state variable constraint.

The state variable constraint

$$S(x;t) = x_5 + d_1 x_4^{d_2} - P^{MAX} \leq 0$$

was handled with the constraining hyperplane technique [4]. Since S is of first order, we thus replaced S with the mixed state-control variable constraint

$$\frac{dS}{dt}(x,u;t) + A_1 S(x;t) \leq 0 \qquad A_1 > 0 \tag{5.13}$$

Differentiating S with respect to t, we get

$$\frac{dS}{dt} = \frac{dx_5}{dt} + d_1 d_2 x_4^{d_2-1} \frac{dx_4}{dt} = u_2 + d_1 d_2 x_4^{d_2-1} f_4(x,u)$$

and thus the mixed state-control variable constraint (5.13) becomes

$$u_2 + d_1 d_2 x_4^{d_2-1} f_4(x,u) + A_1\left(x_5 + d_1 x_4^{d_2} - P^{MAX}\right) \leq 0 \tag{5.14}$$

The parameter A_1 was set equal to 10, which proved to give a sufficiently accurate approximation of $S(x;t) \leq 0$.

5.1.5. Minimization of the Hamiltonian.

By converting the problem into a singular problem, the minimization of the Hamiltonian is considerably simplified compared to Section 4. With the ε-$\alpha(\cdot)$ algorithm we have

$$H(x,u,V_x;t) = \varepsilon_1\left(u_1(t) - \alpha_1(t)\right)^2 + \varepsilon_2\left(u_2(t) - \alpha_2(t)\right)^2 + \\ + \sum_{i=1}^{5} V_{x_i} f_i(x,u)$$

Thus, H is strictly convex in u, and the minimization can be done analytically. In particular

$$u_1^*(t) = \alpha_1(t) - V_{x_4} \cdot \frac{\partial f_4}{\partial u_1}/2\varepsilon_1$$

$$u_2^*(t) = \alpha_2(t) - V_{x_5}/2\varepsilon_2$$

when none of the control variable constraints are active. When any of the constraints (5.9) or (5.14) is active, the quadratic form of H implies that it is still possible to give an explicit expression for the minimizing control variables. Thus, the execution time for the minimization of H is considerably reduced, and the errors due to the discretization of the admissible control region are eliminated.

5.2. Optimal Solutions.

5.2.1. Optimal solution for $t_f = 10.0$.

With the techniques outlined above, the optimal solution was computed for the terminal time $t_f = 10.0$. The following parameters were used:

$\varepsilon_1 = 0.001$

$\varepsilon_2 = 0.01$

$k_a = 10.0$

$k_b = 10.0$

The computed optimal trajectories are shown in Fig. 5.1, and the optimal control strategies together with the optimal termperature and pressure strategies are shown in Figs. 5.2 and 5.3. The optimal hemicellulose yield was $x_2(t_f) = 6.97\%$, and comparing with Fig. 4.10 it can be seen that this is only slightly less than the optimal yield for the case when the control change rates are unconstrained. It should also be noticed that the pressure control strategy is similar in both cases. Further computational aspects are discussed in [5], where also other cost functionals are considered.

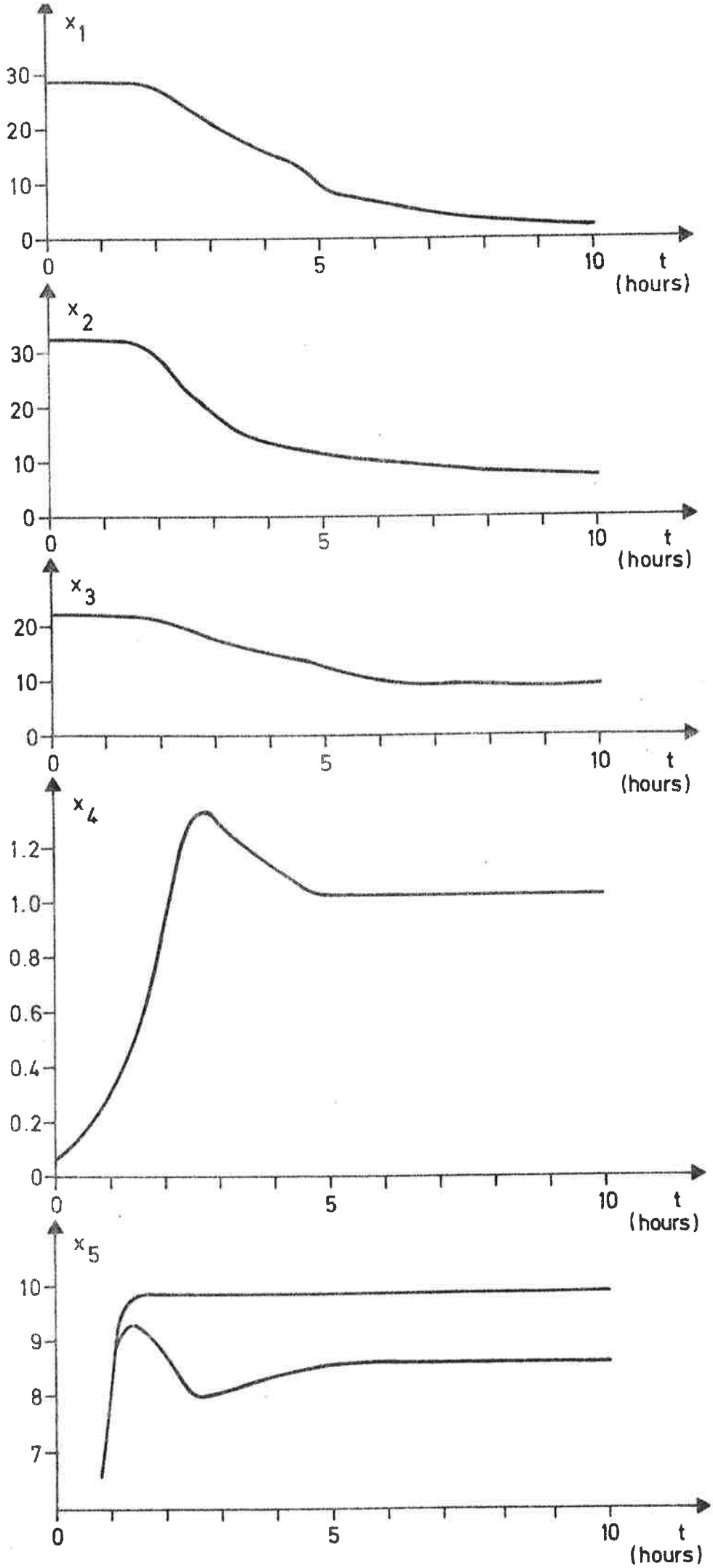

Fig. 5.1 - Computed optimal trajectories for $t_f = 10.0$.

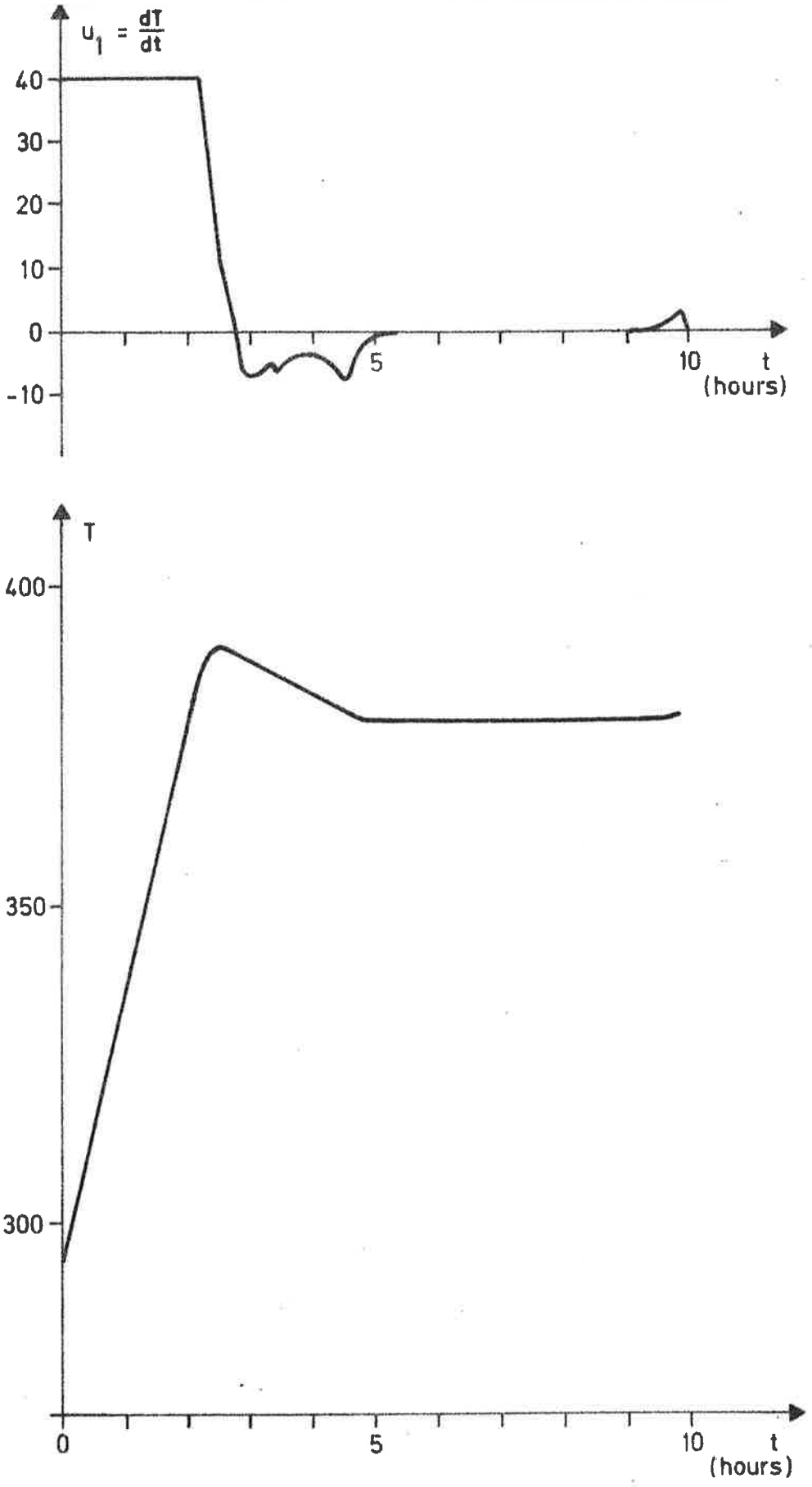

Fig. 5.2 - Computed optimal control variable $u_1(t)$ (=dT/dt) and computed optimal temperature strategy for $t_f = 10.0$.

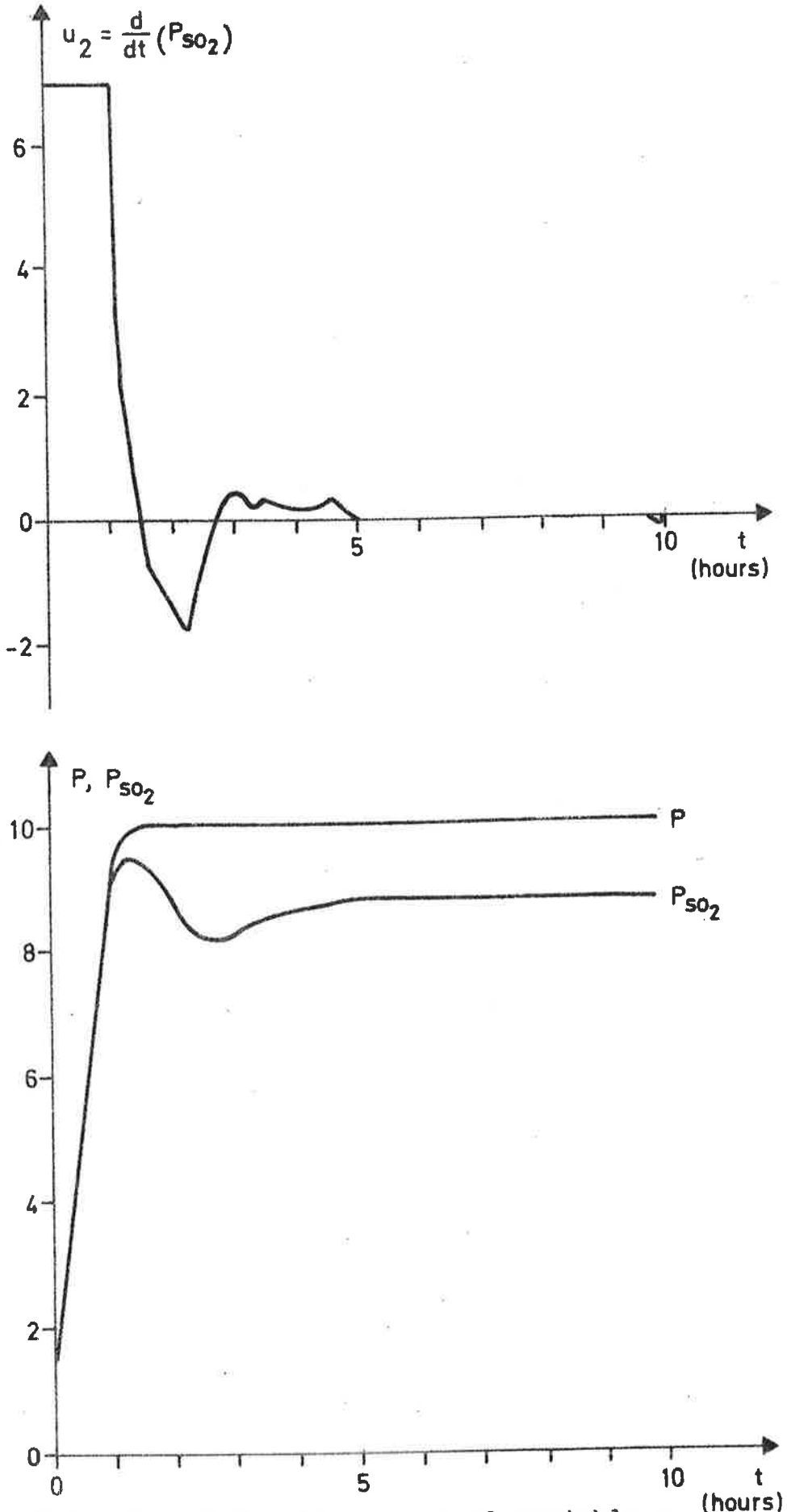

Fig. 5.3 - Computed optimal control variable u_2 (= dp_{SO_2}/dt) and computed optimal pressure strategy for t_f = 10.0.

5.2.2. Reduction of the temperature at the end of the cook.

Most of the different quality aspects are very difficult to include in a mathematical formulation of the problem. However, it is known by experience that a reduction of the temperature at the end of the cook has a favourable influence on the quality of the pulp. This aspect can be included in the problem by adding the quadratic term $k_c x_4^2(t_f)$ to the cost functional. By choosing a large value of the parameter k_c, the terminal optimal temperature will thus be reduced. However, this also implies that the optimal yield $x_2(t_f)$ is reduced, and thus in practice the best choice of k_c is determined by a trade-off between quality and yield.

In Fig. 5.4 the optimal temperature strategies and the optimal yields are shown for different values of k_c. Besides, the optimal yield is shown as a function of the temperature at the end of the cook. The corresponding optimal trajectories for $k_c = 50$ are shown in Fig. 5.5.

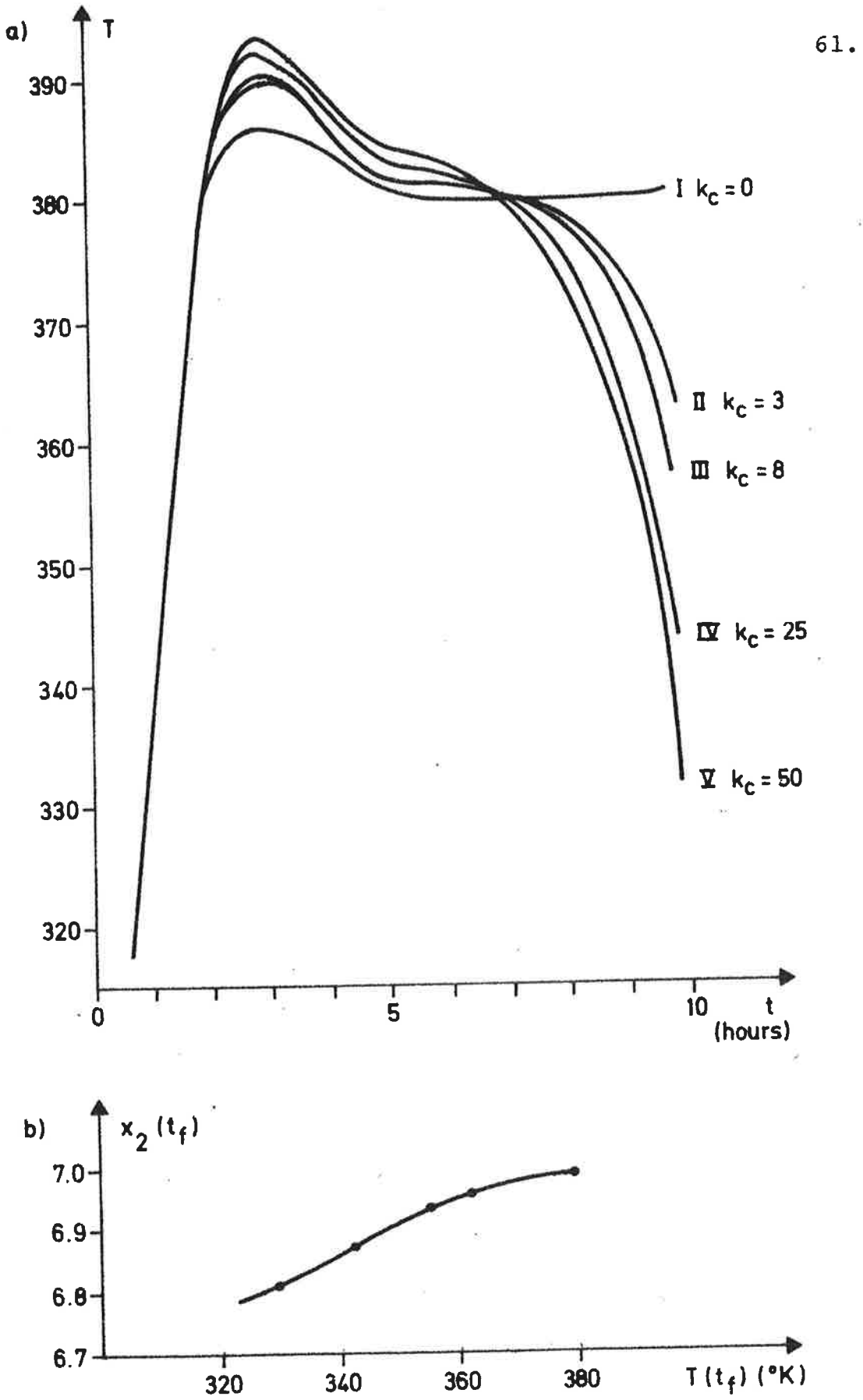

Fig. 5.4 - a) Computed optimal temperature strategies for different values of the parameter k_c.
b) Optimal yield $x_2(t_f)$ as a function of the temperature at the end of the cook.

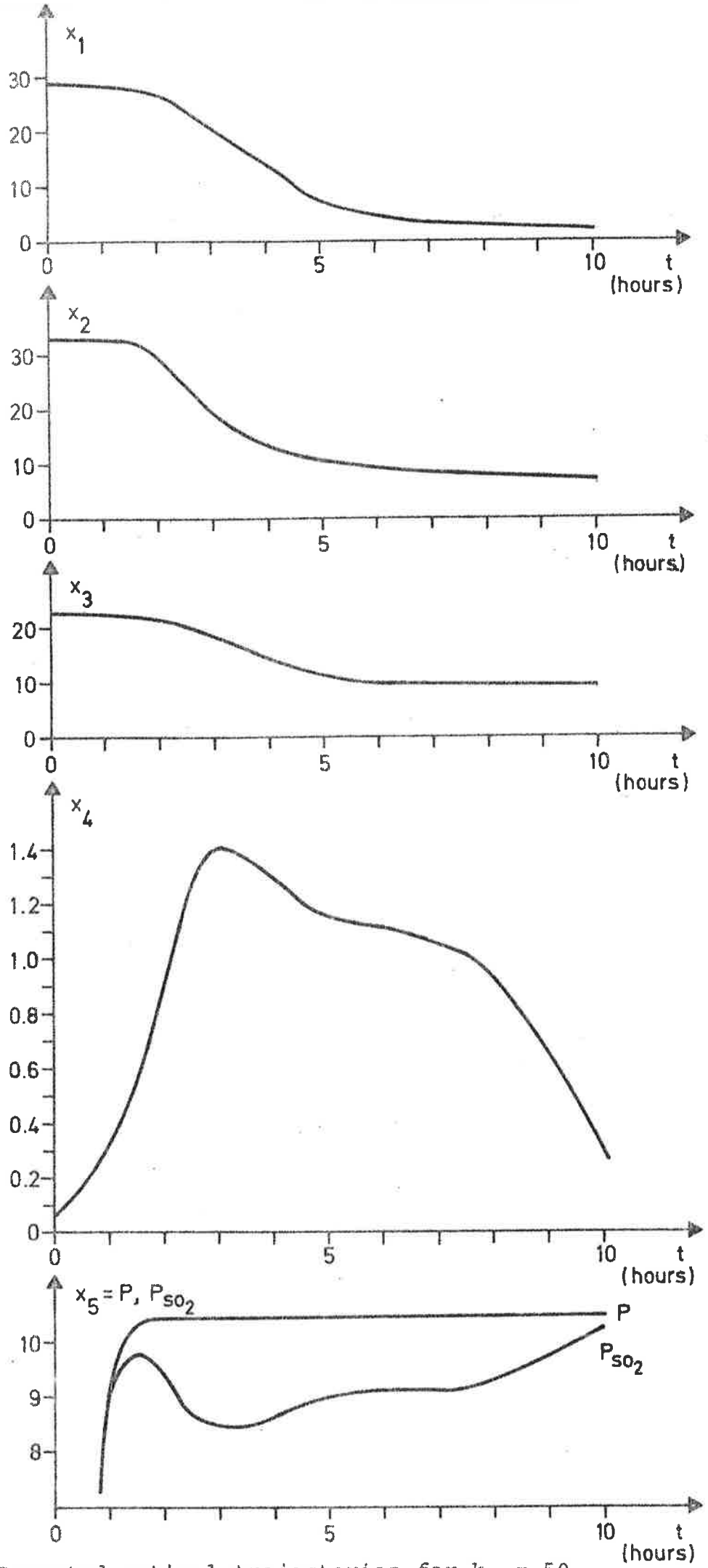

Fig. 5.5 - Computed optimal trajectories for $k_c = 50$.

6. OPTIMAL CONTROL OF MODEL II.

We will in this section use a slightly different model for the sulfite cooking process. The formation of strong acids will be described by (2.8), which is somewhat more accurate in accounting for experimental data than (2.4). It turns out, however, that the optimal control strategies and corresponding trajectories (apart from the concentration of strong acids) are affected only to a small extent by the change of model.

The constraints on control change rates and the terminal constraints are in this section changed to values that are commonly used in practice. Furthermore, the optimal control strategies and optimal values of the cost functional are studied as functions of various parameters.

The optimization problem posed in this section is very similar to that of Section 5. Thus, it is singular and it has state variable constraints as well as control variable and terminal constraints. In fact, it turns out that the posed problems are quite straightforwardly solved applying the technique of the previous sections.

Therefore we will here just give a mathematical formulation of the new optimization problem (Section 6.1) and show the optimal control strategies and corresponding trajectories (Section 6.2).

6.1. Preparations.

6.1.1. The mathematical model.

The formation of strong acids, $[SA^-]$ is described by (2.8):

$$\frac{d}{dt}[SA^-] = \left\{k^o_{SA} \exp(-E_{SA}/T)/v\right\}[SA^-]^a [HSO_3^-]^b [H^+]^c$$

The values of the constants are given in (2.9). The other equations remain unaltered from Section 5.1.

Introduce the state variables

$x_1 = [L]$	(%)	cf. Section 4.1.1
$x_2 = [C]$	(%)	
$x_3 = [SA^-] \cdot 100$	($[SA^-]$ in moles/lit.)	
$x_4 = 10^4 \cdot \exp(-3500/T)$	(T in ^oK)	
$x_5 = p_{SO_2}$	(bar)	

The coefficients in the definition of x_3 and x_4 have been chosen to make all state variables vary in the same range.

As control variables are chosen

$$u_1 = \frac{d}{dt} T$$

and

$$u_2 = \frac{d}{dt} P$$

(Notice that u_2 is the derivative of the total pressure and not as in Section 5 of the partial pressure p_{SO_2}. This

is since it is more natural to have limits on the change rate of the total pressure, when the pressure is decreased. In this section we will have terminal constraints for the pressure.)

The system equations then are

$$\frac{dx_1}{dt} = f_1(x,u) = - k_1(x) x_4^{\ell_1(x)} \cdot x_1^{\ell_4(x)} [\, r_1(x)]^{\ell_5(x)} \cdot$$

$$\cdot [\, r_2(x)]^{\ell_6(x)}$$

$$\frac{dx_2}{dt} = f_2(x,u) = - k_2 x_4^{\ell_2} x_2^{\ell_7} [\, r_2(x)]^{\ell_8} \qquad (6.1)$$

$$\frac{dx_3}{dt} = f_3(x,u) = k_6 x_4^{\ell_{13}} x_3^{\ell_{14}} [\, r_1(x)]^{\ell_{15}} [\, r_2(x)]^{\ell_{16}}$$

$$\frac{dx_4}{dt} = f_4(x,u) = x_4 [{}^e\log(10^4/x_4)]^2 u_1/3500$$

$$\frac{dx_5}{dt} = f_5(x,u) = u_2 - k_7 k_8 x_4^{k_8 - 1} f_4(x,u)$$

The initial conditions are

$x_1(0) = 28.$

$x_2(0) = 32.$

$x_3(0) = 0.0001$

$x_4(0) = 10^4 \exp(-3500/333)$ $\quad (T(0) = 333^{\circ}K)$

$x_5(0) = 1.80883$ $\quad (P(0) = 2$ bar$)$

The variables $r_1(x)$ and $r_2(x)$ are defined in Section 5.1.1.

The numerical values of the constants are given in (5.4), (5.5) and (5.6).

In addition

$$k_6 = [0.98815 \cdot 10^{12}/(v-10^{\frac{4}{3}}\ell_1)] \cdot 100^{1.4296}$$

$$k_7 = 10^{5.882-4k_8}$$

$$k_8 = 2198\ {}^{e}\log(10)/3500$$

$$\ell_{13} = 10484/3500 \qquad (6.2)$$

$$\ell_{14} = -0.4296$$

$$\ell_{15} = 0.6298$$

$$\ell_{16} = 0.5537$$

6.1.2. The cost functional and the constraints.

The cost functional is the same as before, i.e.

$$J = - x_2(t_f)$$

where t_f is the a priori fixed terminal time.

The terminal constraints are

$$\psi_1(x(t_f)) = x_1(t_f) - 2.0 = 0$$

as before. It will now also be added

$$\psi_2(x(t_f)) = k_{\psi_2}(x_5(t_f) + k_1 x_4(t_f)^{k_8} - 2.5) = 0$$

which corresponds to $P(t_f) = 2.5$ bar.

Also the terminal temperature must satisfy $T(t_f) \leq 373^{\circ}K$. Therefore a constraint

$$\psi_3(x(t_f)) = k_{\psi_3}[x_4(t_f) - 10^4 \exp(-3500/373)] = 0$$

is introduced in case the unconstrained optimal solution gives a terminal temperature greater than $373^{\circ}K$.

The coefficients k_{ψ_2} and k_{ψ_3} are chosen as

$$k_{\psi_2} = 0.25$$

$$k_{\psi_3} = 0.5$$

to attain proper accuracies in the test $||\psi|| < \eta$.

The control variables have to satisfy

$$u_1^{MIN} \leq u_1(t) \leq u_1^{MAX}$$

$$u_2^{MIN} \leq u_2(t) \leq u_2^{MAX}$$

for all $t \in [0, t_f]$

with, unless otherwise stated,

$u_1^{MIN} = -30$ $\quad u_1^{MAX} = 30$ (degrees Kelvin/hour)

$u_2^{MIN} = -8$ $\quad u_2^{MAX} = 8$ (bar/hour)

Finally, as in Section 5.1.2 we have the following state variable constraints

$$1 \leq P \leq P^{MAX}$$

$$T^{MIN} \leq -350\ln\left[e\log\left(10^{-4}x_4\right)\right]^{-1} \leq T^{MAX}$$

It turns out that the second constraint is never active and can be omitted. The first one gives

$$S(x,t) = x_5 + k_7 x_4^{k_8} - P^{MAX} \leq 0$$

Unless otherwise stated P^{MAX} will be 7 bar.

As in Section 5.1 the cost functional will in view of the singularity of the problem, and because of the terminal constraints be modified to

$$J = -k_a x_2(t_f) + \int_0^{t_f} \left[\varepsilon_1\left(u_1(t) - \alpha_1(t)\right)^2 + \right.$$

$$\left. + \varepsilon_2\left(u_2(t) - \alpha_2(t)\right)^2\right]dt + k_b\left(x_1(t_f) - 2\right)^2 +$$

$$+ k_c\left[x_5(t_f) + k_7 x_4(t_f)^{k_8} - 2.5\right]^2 +$$

$$+ k_d\left[x_4(t_f) - 10^4 \exp(-3500/373)\right]^2$$

where k_d is nonzero only in case ψ_3 is active.

6.2. Optimal Solutions.

With the technique outlined in Sections 4 and 5 optimal control strategies were computed for a number of cases.

The optimal solution for the values of the parameters given above and terminal time t_f = 7 hours is shown in Fig. 6.1. Here also a simulation of a control strategy usually applied in practice is shown.

The decrease of the cost functional obtained when using the optimal control is indeed very small. This obviously is due to the fact that the constraints are active most of the time.

From this standard cook of Fig. 6.1 then a number of parameters have been varied, one at a time. These parameters are N (the concentration of Na^+ ions), v (liquor to wood ratio), P^{MAX}, $x_1(t_f)$, t_f and $u_1^{MAX,MIN}$.

In Fig. 6.2 is shown optimal solutions for various values of P^{MAX}.

Finally, in Fig. 6.3 the optimal value of the cost functional (i.e. $x_2(t_f)$) is shown as a function of the aforementioned parameters.

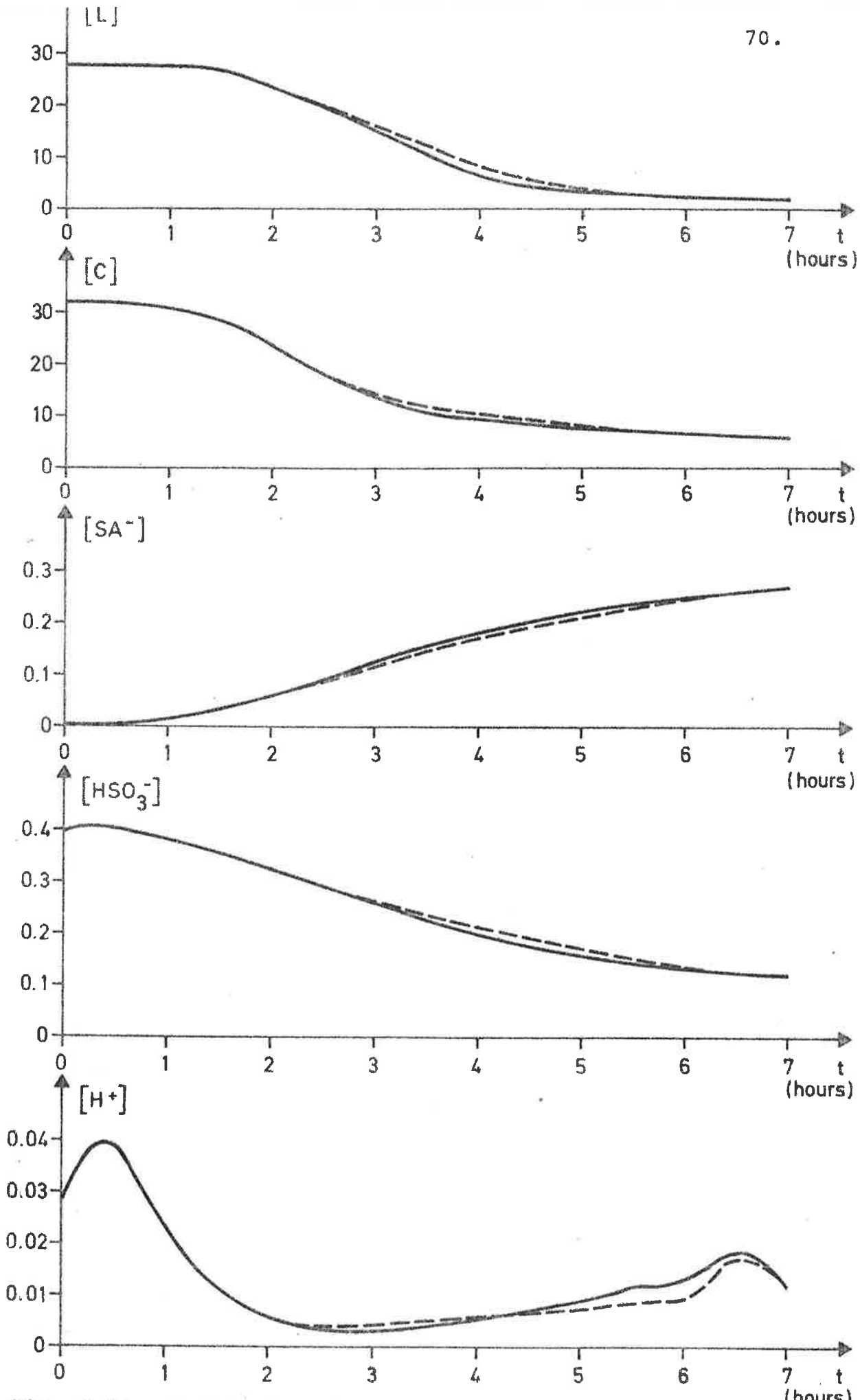

Fig. 6.1a - Solid line: Computed optimal trajectories. Dashed line: Trajectories for control strategy used in practice.

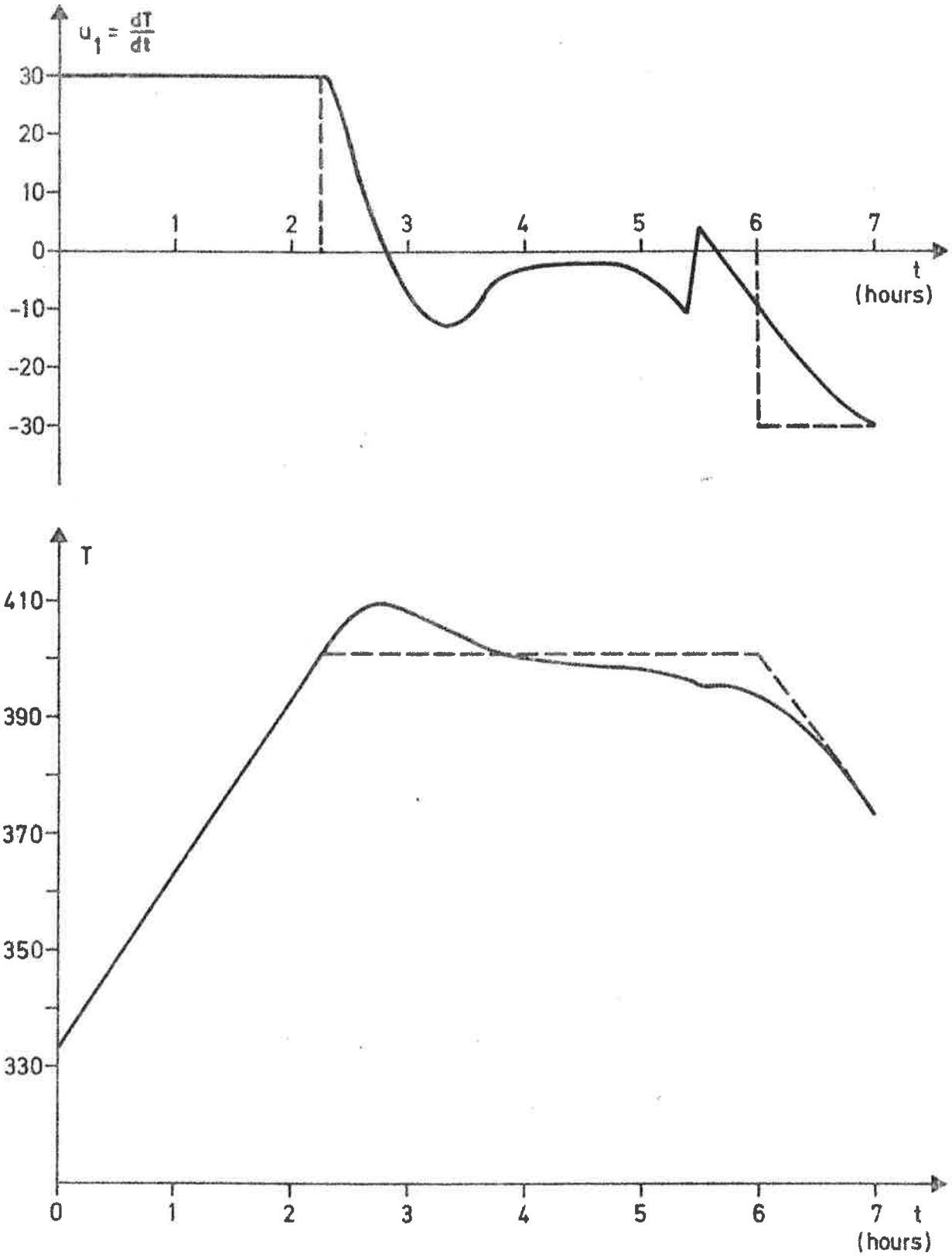

Fig. 6.1b:- Solid line: Computed optimal control strategy.
Dashed line: Control strategy used in practice.

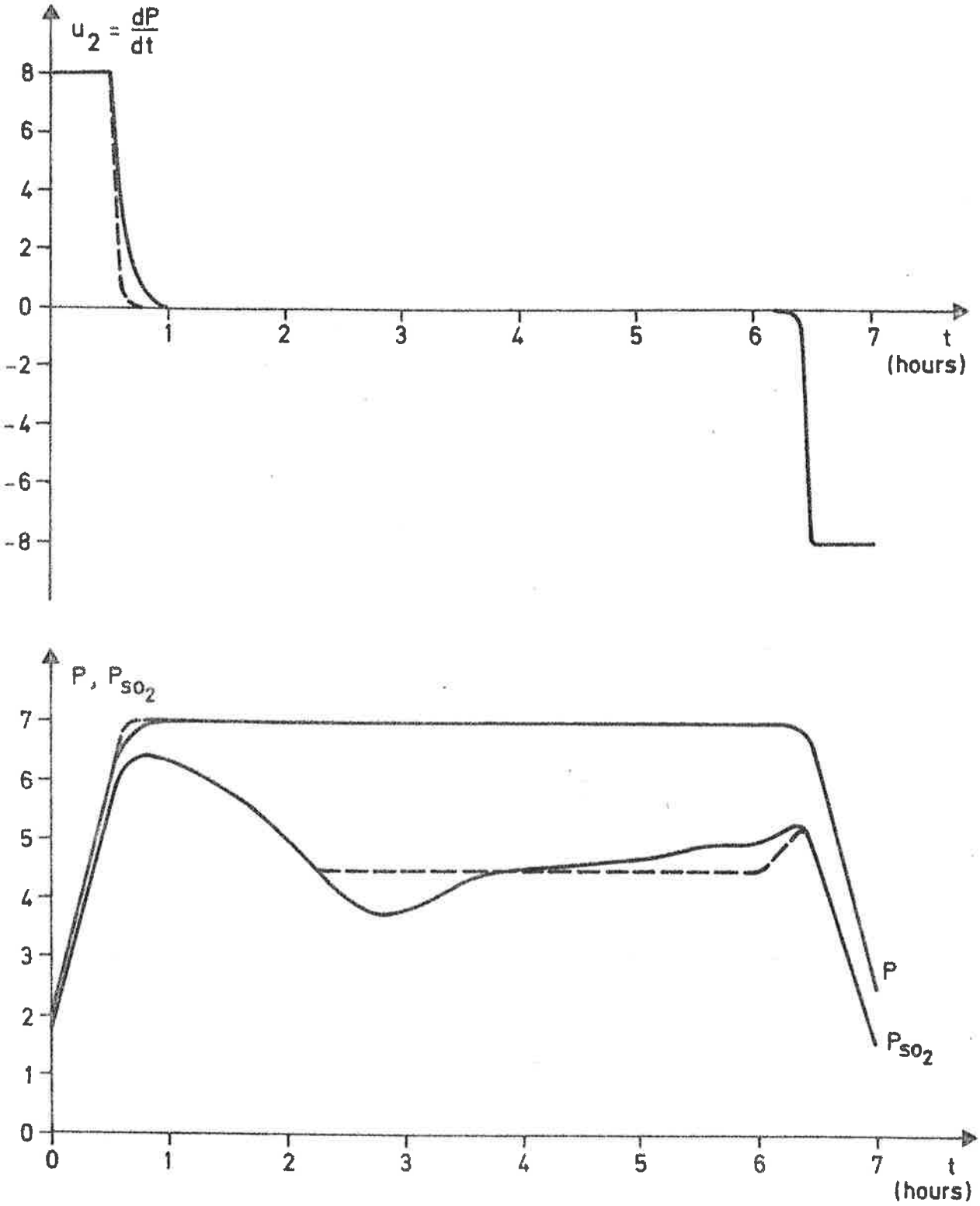

Fig. 6.1c - Solid line: Computed optimal control strategy.
Dashed line: Control strategy used in practice.

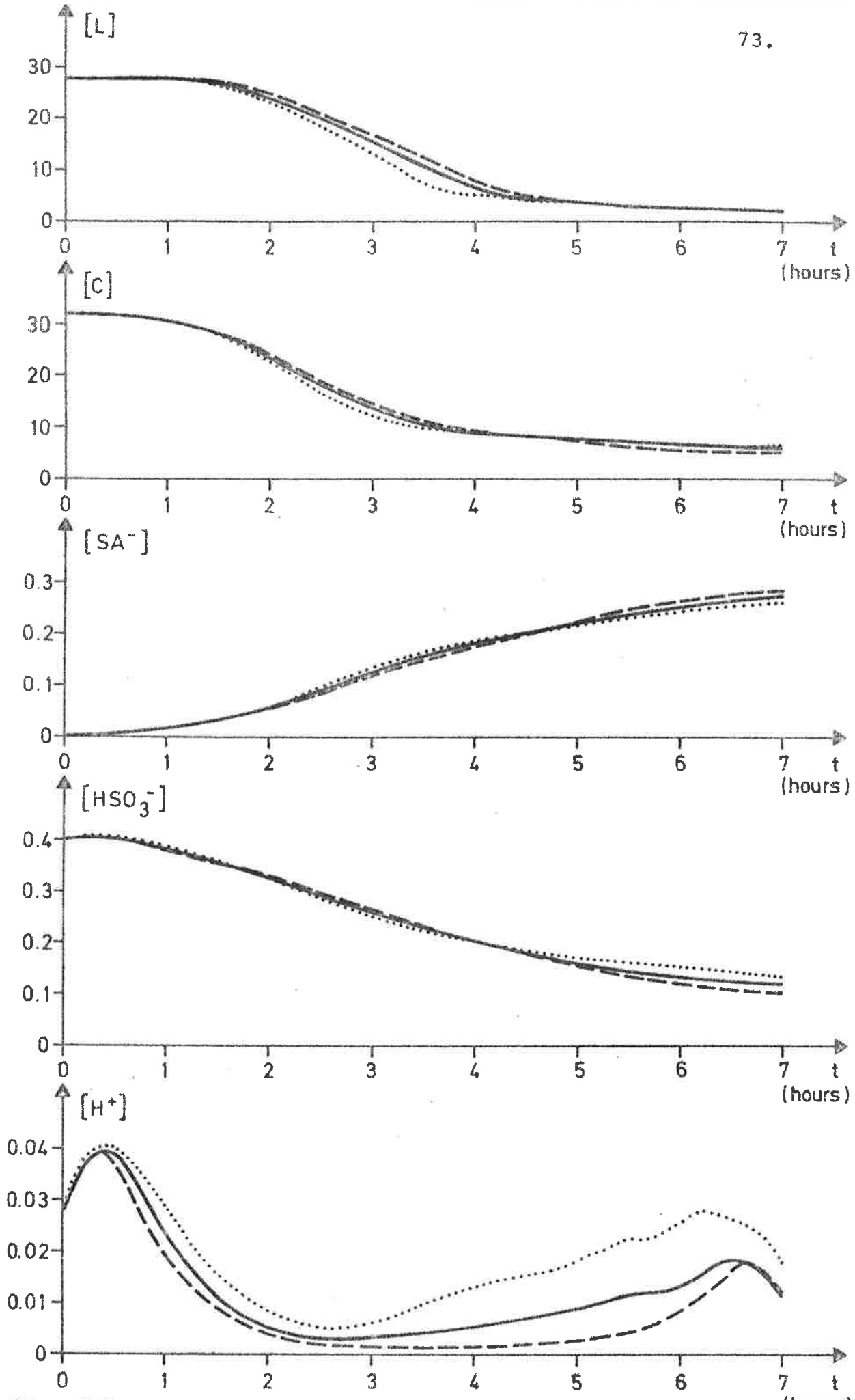

Fig. 6.2a - Computed optimal trajectories for P_{MAX} = 7 bar (solid line), 9 bar (dotted line) and 6 bar (dashed line).

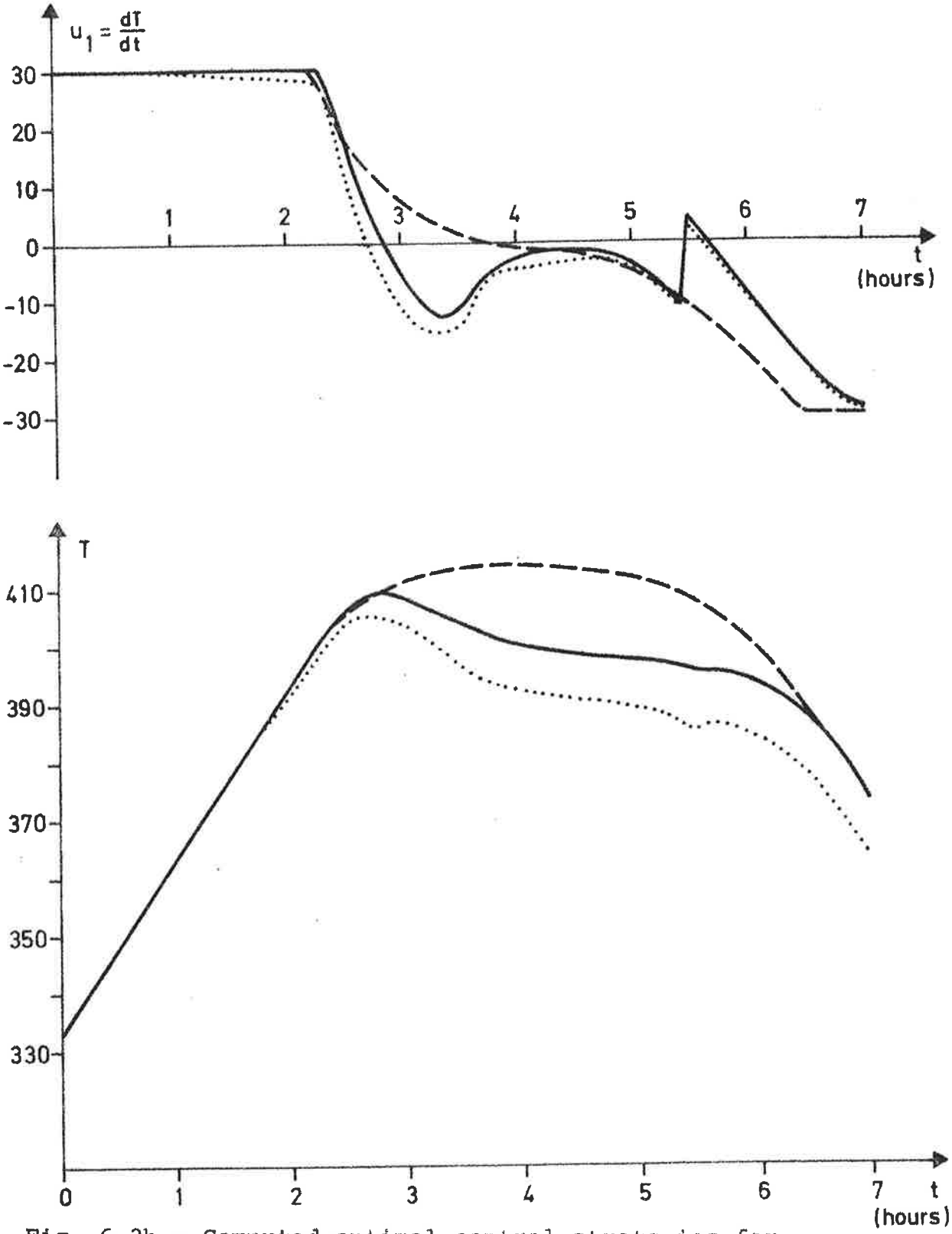

Fig. 6.2b - Computed optimal control strategies for p_{MAX} = 7 bar (solid line), 9 bar (dotted line) and 6 bar (dashed line).

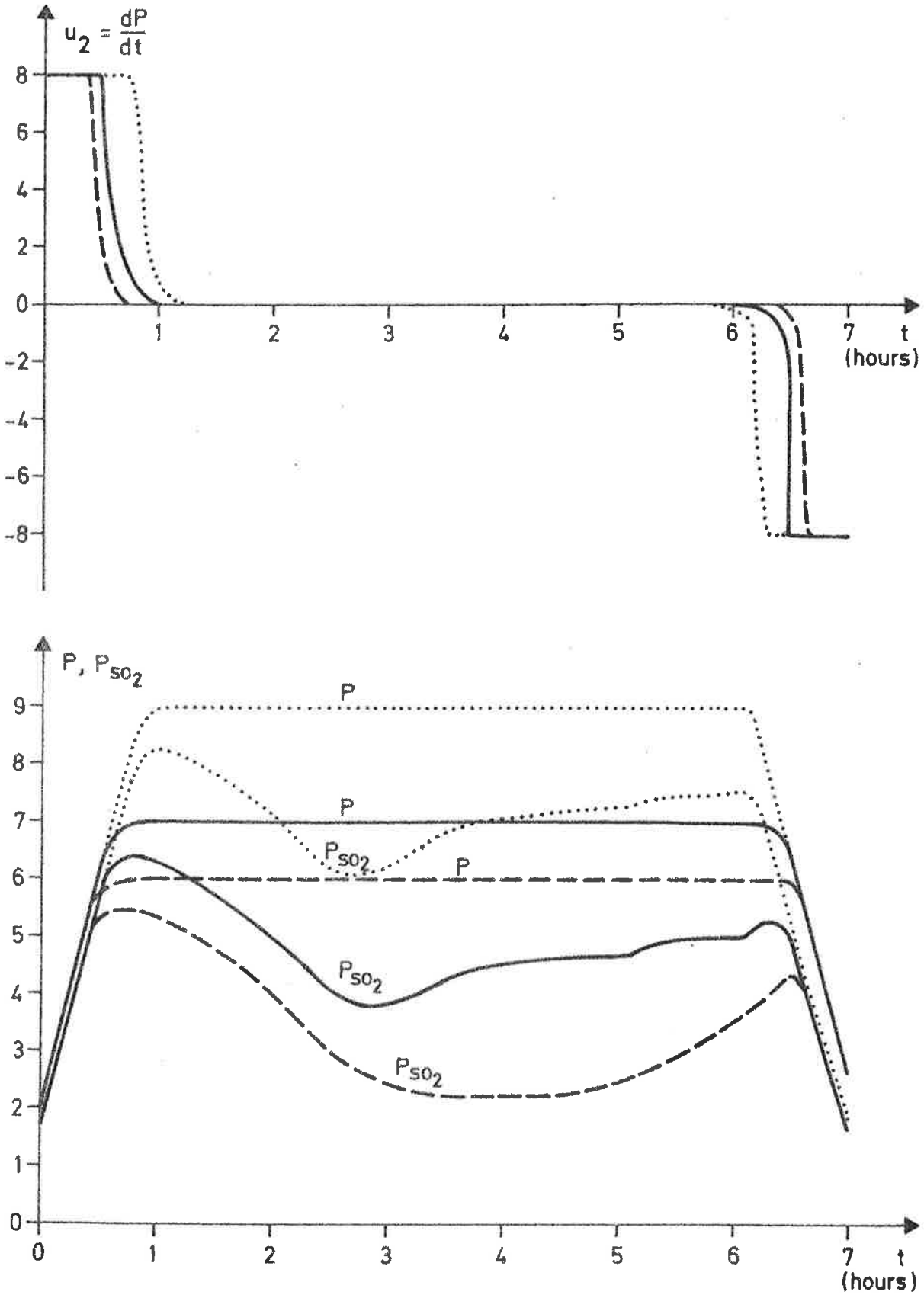

Fig. 6.2c - Computed optimal control strategies for P_{MAX} = 7 bar (solid line), 9 bar (dotted line) and 6 bar (dashed line).

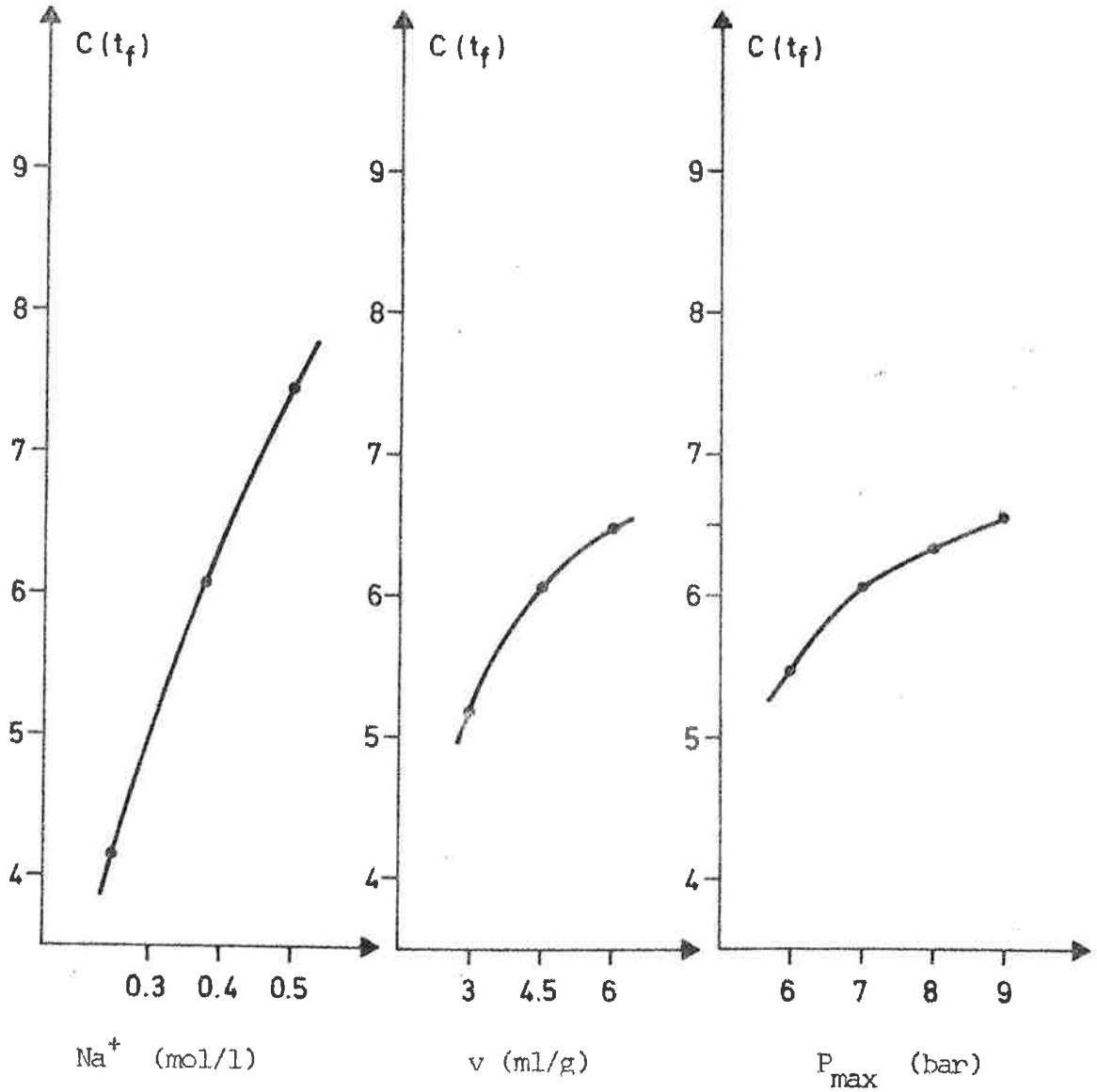

Fig. 6.3a- Optimal value (in %) of $C(t_f)$ as a function of various variables. Not varied variables have the values given in Section 6.1.

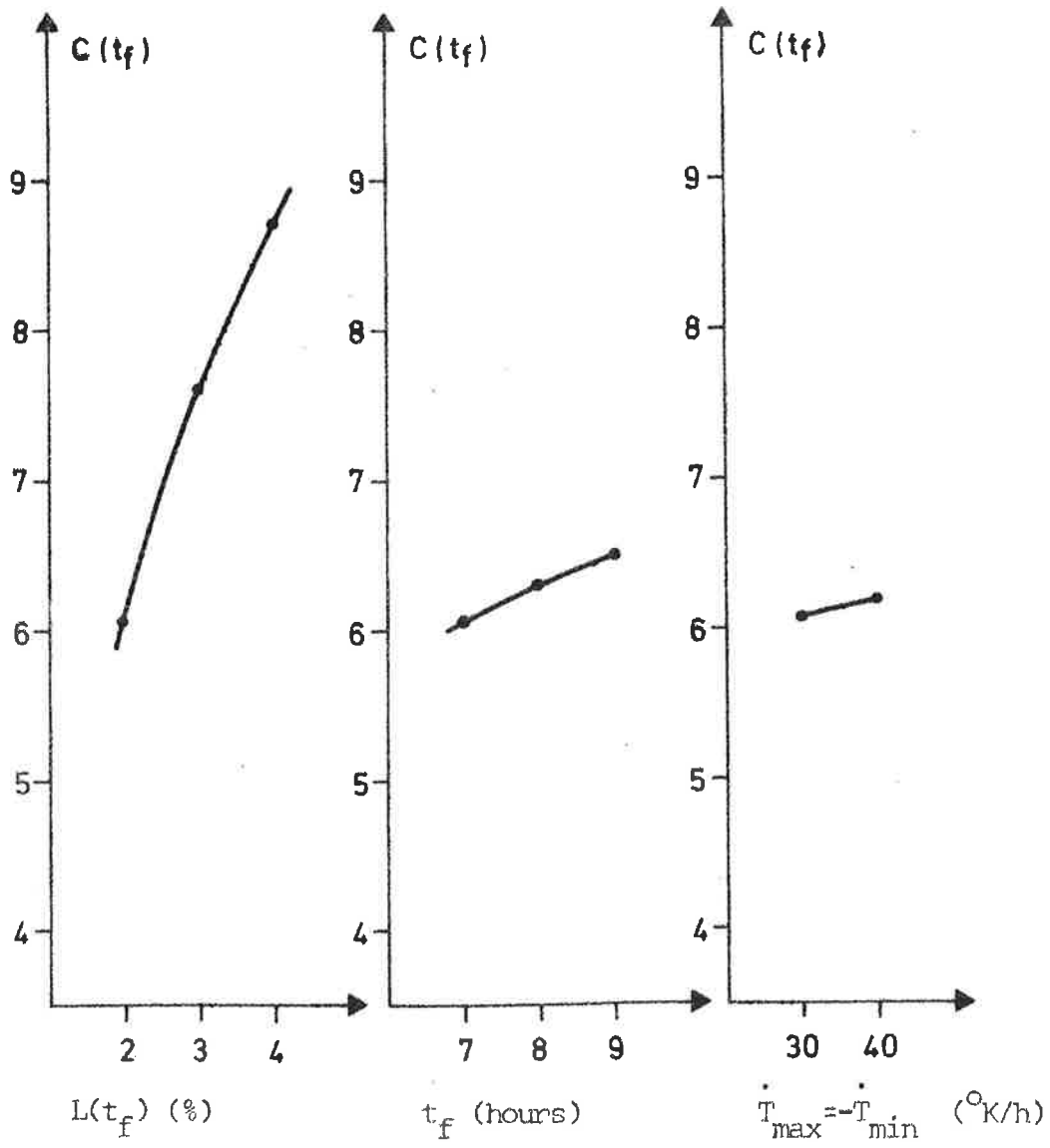

Fig . 6.3b - Optimal value (in %) of $C(t_f)$ as a function of various variables. Not varied variables have the values given in Section 6.1.

7. REFERENCES.

[1] A.E. Bryson and Y.C. Ho: "Applied Optimal Control", Blaisdell, Waltham, 1969.

[2] D.H. Jacobson, S.B. Gerschwin and M.M. Lele: "Computation of Optimal Singular Controls", IEEE Trans. Automatic Control, Vol. 15, 1970.

[3] D.H. Jacobson and D.Q. Mayne: "Differential Dynamic Programming", American Elsevier Publishing Comp. New York, 1970.

[4] K. Mårtensson: "New Approaches to the Numerical Solution of Optimal Control Problems", Research Report 7206, Division of Automatic Control, Lund Institute of Technology, Lund, 1972.

[5] L.O. Nilsson: "Optimal Control of the Acid Sulfite Cooking Process" (in Swedish), Report RE-108, Division of Automatic Control, Lund Institute of Technology, Lund, 1972.

[6] N.H. Schöön: "Kinetic Aspects of the Acid Sulfite Cooking Process", Research Report, Department of Chemical Reaction Engineering, Chalmers University of Technology, Gothenburg, 1972.

[7] N.H. Schöön and B. Hagberg: "Kinetic Aspects of the Acid Sulfite Cooking Process, Parts I & II", to appear in Svensk Papperstidning.

[8] B. Hagberg and N.H. Schöön: "Kinetik och simulering av sulfitkokningsprocessen",rapport över STU-projekt nr 68-308-n (1970). (In Swedish).